NASA CONTRACTOR
REPORT

NASA CR-161889

FEASIBILITY STUDY -- ATMOSPHERIC GENERAL CIRCULATION EXPERIMENT, VOLUME I

Edited by R. J. Homsey
General Electric Company
Space Systems Division
P. O. Box 8555
Philadelphia, Pennsylvania 19101

Final Report - Volume I

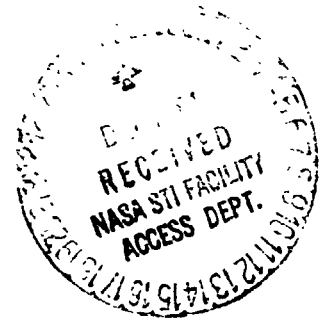

September 1, 1981

(NASA-CR-161889-Vol-1) FEASIBILITY STUDY: ATMOSPHERIC GENERAL CIRCULATION EXPERIMENT, VOLUME 1 Final Report (General Electric Co.) 97 p HC A05/MF A01 CSCL 22A

N82-15064

G3/12 Unclas 06426

Prepared for

NASA - George C. Marshall Space Flight Center
Marshall Space Flight Center, Alabama 35812

1. Report No. NASA CR-161889	2. Government Accession No.	3. Recipient's Catalog No.

4. Title and Subtitle

Feasibility Study — Atmospheric General Circulation Experiment, Volume I

5. Report Date September 1, 1981

6. Performing Organization Code

7. Author(s)

Edited by R. J. Homsey

8. Performing Organization Report No.

10. Work Unit No.

9. Performing Organization Name and Address

General Electric Company
Space Systems Division
P.O. Box 8555
Philadelphia, Pennsylvania 19101

11. Contract or Grant No. NAS8-34049

12. Sponsoring Agency Name and Address

National Aeronautics and Space Administration
Washington, D.C. 20546

13. Type of Report and Period Covered Contractor Final Report - Volume I

14. Sponsoring Agency Code

15. Supplementary Notes

Prepared under the technical monitorship of the Atmospheric Sciences Division, Space Sciences Laboratory, Science and Engineering Directorate, NASA/Marshall Space Flight Center

16. Abstract

The near-zero gravity environment of Spacelab presents the opportunity to perform laboratory model experiments of large-scale planetary circulations in true spherical geometry. The Atmospheric General Circulation Experiment (AGCE) has been proposed to conduct such experiments in Spacelab using a rotating fluid flow cell assembly. The study, conducted in close cooperation with personnel from the NASA-MSFC, analytically investigates the key technical areas affecting the feasibility of the design and operation of the AGCE. The areas investigated include materials for the flow cell assembly, thermal design, high voltage power supply design, effective retrieval and handling of experiment data and apparatus configuration. Several materials, DMSO and m-tolunitrile, were selected as candidate fluids for the flow cell principally for their high dielectric constant which permits the high voltage power supply design to be held to 15 kV and still simulate terrestrial gravity. Achievement of a low dissipation factor in the fluid to minimize internal heating from the applied electrical field will depend strongly on purification and handling procedures. The use of sapphire as the outer hemisphere for the flow cell provides excellent viewing conditions without a significant impact on attaining the desired thermal gradients. Birefringent effects from sapphire can be held to acceptably low limits. Visualization of flow fluid is achieved through the motion of a dot matrix formed by photochromic dyes. Two dyes found compatible with the candidate fluids are spiropyran and triarylmethane. The observation of the dot motion is accomplished using a flying spot scanner. The observation of fluid thermal gradients is performed by a four-quadrant detector which measures the translational displacement of the spot generated by the scanner. Moreover, the use of a flying spot scanner while reducing size and weight of the optical system permits direct transmission of data to the Principal Investigator by producing data in electronic form. Operation as well as control of the experiment and its thermal gradients can be done for less than 300 watts. Overall, the AGCE was found to be a feasible experiment fitting well within the constraints for a Spacelab flight. Sufficient flexibility exists in the design parameters to guarantee the achievement of the experimental conditions necessary to explore the onset of baroclinic instabilities in terrestrial-type atmospheres.

Volume I presents the results, and Volume II contains the documentation that contributes to the results given in Volume I. This documentation includes the analysis performed in each technical area, the rationale and substantiation for the hardware design, and design details for the baseline AGCE.

17. Key Words (Suggested by Author(s))

Spacelab zero-gravity experiment
Photochromic flow visualization
Electro-convection
Spherical baroclinic instability

18. Distribution Statement

Unclassified - Unlimited

William C. Kingsbury
J. E. Kingsbury
Acting Director, Space Sciences Laboratory

19. Security Classif. (of this report)	20. Security Classif. (of this page)	21. No. of Pages	22. Price
Unclassified	Unclassified	97	NTIS

MSFC - Form 3292-1 (Rev December 1972) For sale by National Technical Information Service, Springfield, Virginia 22161

ACKNOWLEDGMENTS

The feasibility study for the Atmospheric General Circulation Experiment (AGCE) required a multi-disciplined effort to address the many aspects important to its successful implementation. The necessary skills were drawn not only from experienced personnel within the Space Systems Division of the General Electric Company but also from other experts located at the NASA Marshall Space Flight Center, the Rochester Institute of Technology (RIT), and other components of the General Electric Company.

An expression of appreciation must be particularly given to Dr. W. Fowlis and Mr. B. Schrick of the NASA-MSFC whose technical interaction and guidance throughout the program helped the study team concentrate on the key technical issues affecting experiment feasibility. Also the characterization of fluid flow by Dr. Fowlis was a significant input to the thermal analysis task. Their cooperation is gratefully acknowledged.

The technical contributors who played important roles as part of the study team are:

G.L.Fogal	GE-SSD	Deputy Program Manager, Filtration, Apparatus Configuration, Cost Estimation
S.L.Neste	GE-SSD	Materials for the AGCE Cell, Purification Processes, Fluid Characterization
W.C.Yager	GE-SSD	Optical System Analysis and Design
G.Andres/T.R.Scollon	GE-SSD	Thermal Analysis and Control Design
L.W.Springer/J.Barney	GE-SSD	High Voltage Power Supply Design
W.C.Mosley	GE-SSD	Experiment Control and Data Handling
R.Francis	RIT	Photochromic Dyes Evaluation

D.Shaw	GE-Capacitor Dept.	Dielectric Fluid Properties and Characterization
L.R.Eaton/R.J.Homsey	GE-SSD	Program Manager

The cooperation and professionalism exhibited by everyone made it possible to fully satisfy the study objectives.

TABLE OF CONTENTS

LIST OF ILLUSTRATIONS

LIST OF ILLUSTRATIONS (continued)

LIST OF TABLES

1.0 SUMMARY

An Atmospheric General Circulation Experiment (AGCE), which will model the large-scale circulations of the earth's atmosphere in hemispherical geometry, has been proposed for Spacelab flights. In this experiment the working fluid will be held between two concentric spheres and subjected to a radial electric field in the form of a spherical capacitor. The pole-equator temperature gradient and the large-scale vertical stability of the atmosphere will be modeled by maintaining latitudinal temperature gradients on the spheres and by maintaining the outer sphere warmer than the inner sphere. The rotation of the earth will be modeled by co-rotating the spheres.

Much sophisticated laboratory modeling of the effects of rotation and differential heating on fluids has previously been carried out in cylindrical geometries, and much has been learned which is relevant to the general circulation of the earth's atmosphere. However, these models have serious limitations when attempts are made to extend their results to the spherical geometry of the atmosphere. The principal objectives of the AGCE system are to examine (in the spherical model) the onset of the wave-cyclone (baroclinic) instability, the growth rates and length scales of this instability, and the stationary and time-dependent finite amplitude flows achieved as a consequence of the instability.

Scientific theoretical design studies for the AGCE have shown that it will not be easy to construct an apparatus in which the required baroclinic instability can be realized. Hardware for a similar spherical geophysical fluid dynamic experiment is currently under development for NASA by the Aerojet General Corporation. This experiment, the Geophysical Fluid Flow Cell (GFFC), is concerned with modeling convectively unstable circulations as are found in

stars. In the GFFC the inner sphere will always be maintained at a higher temperature than the outer sphere.

Although the science in general and the fluid dynamic capabilities in particular of the GFFC experiment and the AGCE are essentially different, the engineering and the hardware for both experiments have much in common.

This study concentrates on those areas of technology and design which are unique to the AGCE in order to assess its feasibility. The topics of concern for the feasibility study include the selection of materials for the experiment observation, thermal design to control experiment conditions, experiment configuration for use on Spacelab and cost of implementation. In establishing the design for the AGCE, GFFC design experience was used whenever possible.

The results of the study clearly establish the feasibility of the AGCE as a Spacelab flight experiment. The AGCE as it might appear in a single experiment rack is depicted in Figure 1.1-1 by a wooden model illustrating the main subsystems. The experiment mechanical assembly in the lower position contains the fluid cell in a sealed nitrogen atmosphere. The bulk of the associated electronics is in the upper position.

The enclosure subassembly, Figure 1.1-2, is designed to contain the optical scanner assembly for data acquisition, the ultraviolet optical assembly for dye marker matrix generation and the cooling duct for the thermoelectric module (TEM) located on the pole of the fluid cell.

The turntable subassembly, Figure 1.1-3, contains the majority of mechanical components required to perform the experiment.

The heart of the AGCE is the flow cell assembly shown in Figure 1.1-3. It

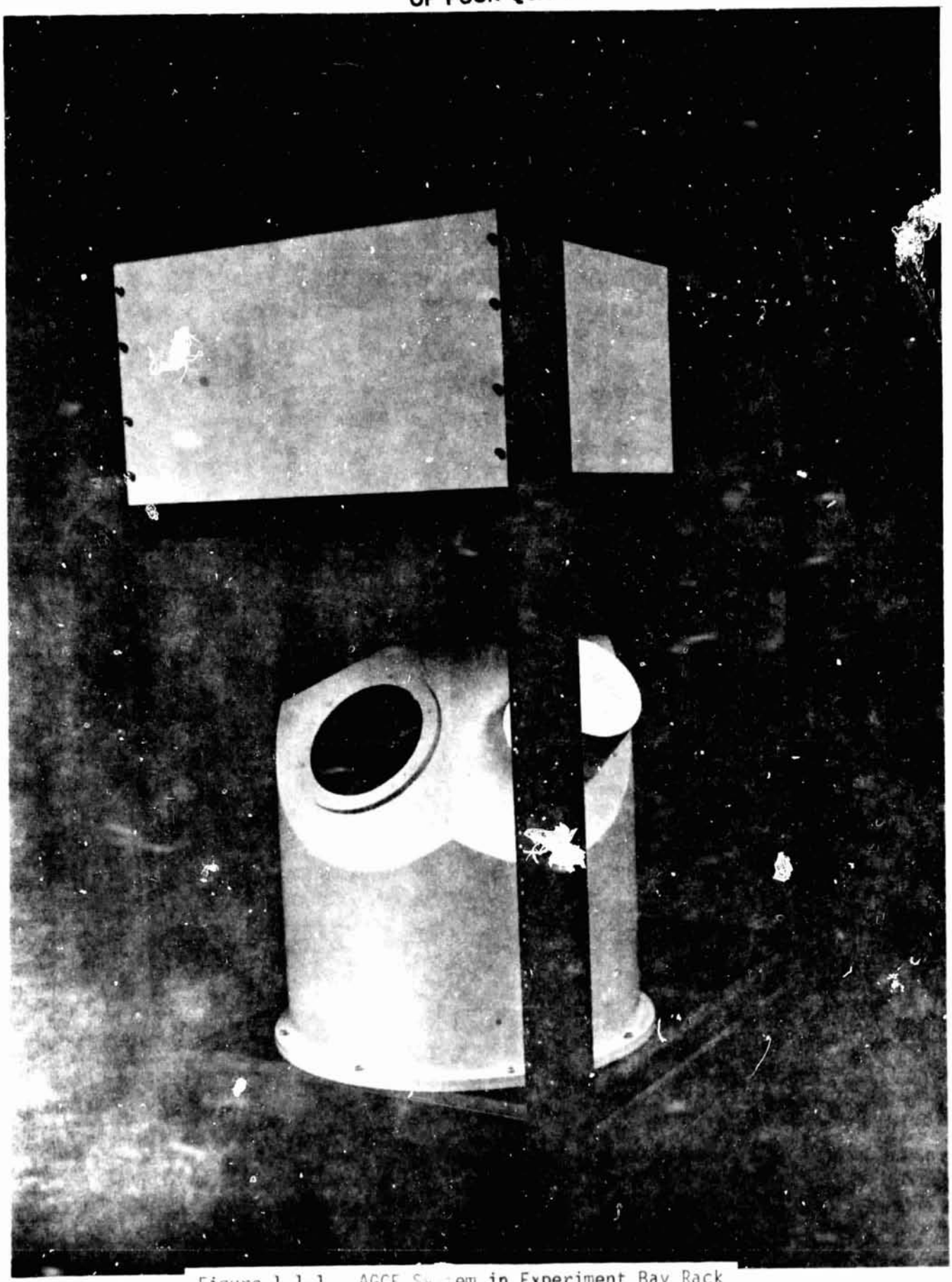

Figure 1.1-1. AGCE System in Experiment Bay Rack

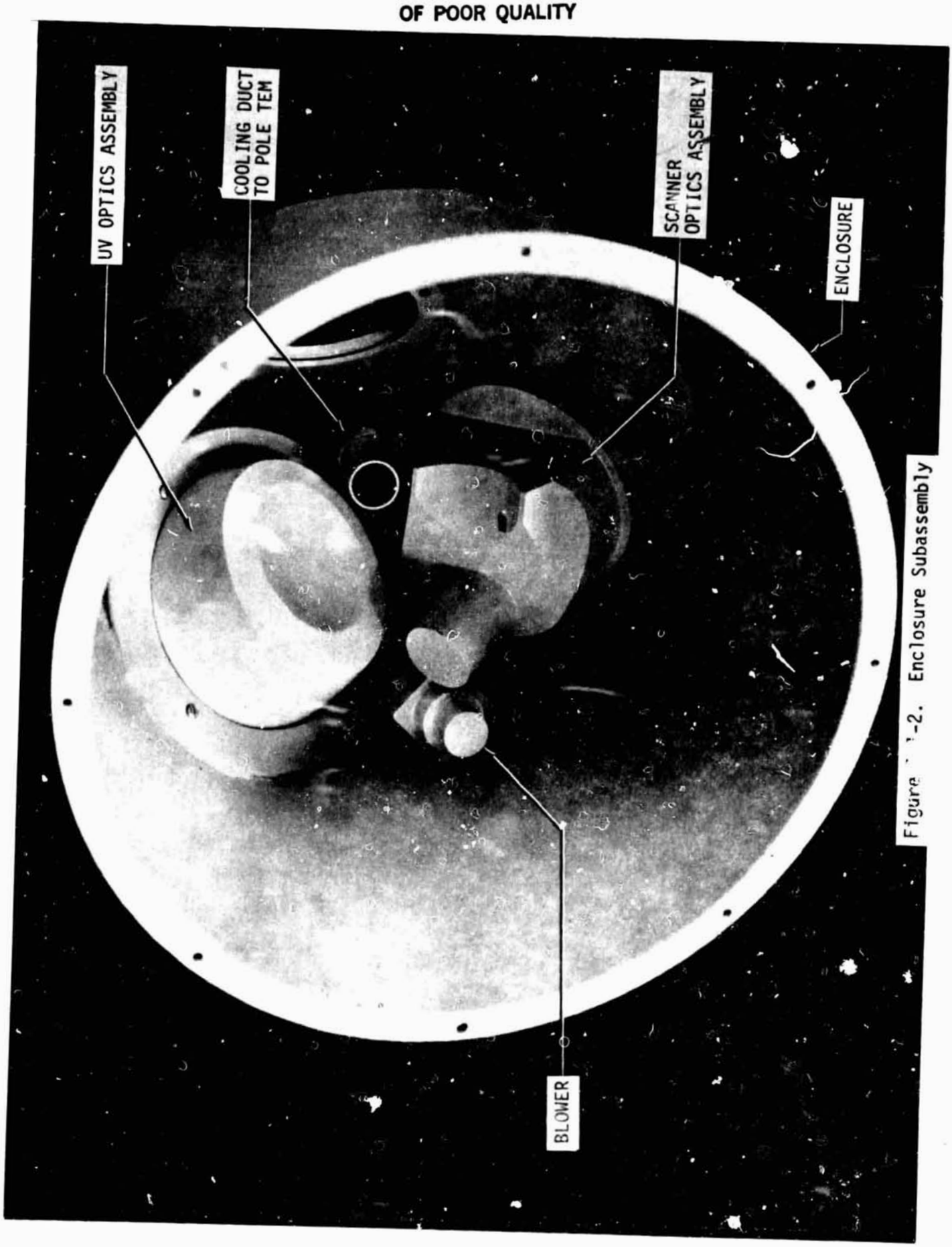

Figure 1-2. Enclosure Subassembly

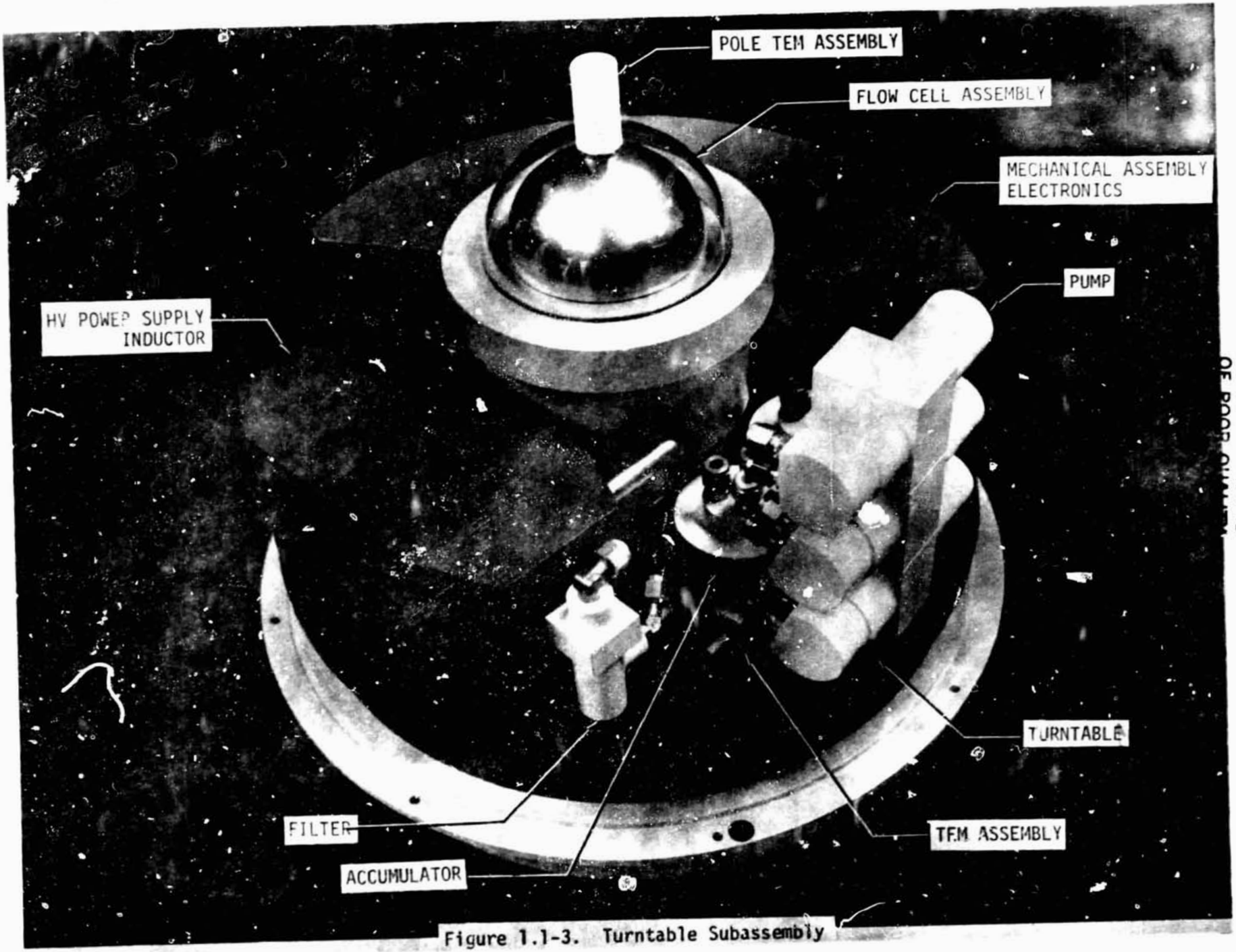

Figure 1.1-3. Turntable Subassembly

received the most attention during the assessment of the AGCE feasibility. The identification of appropriate fluids to be used to simulate atmospheric circulation under the influence of gravity simulated by a radial electric field was one of the most critical challenges in the study. Following a broad survey of fluids and fluid properties, several candidates emerged with acceptable values for their dielectric constant, viscosity and power dissipation factor while still being compatible with useble photochromic dyes. The fluids, having dielectric constants above 40, are dimethylsulfide (DMSO) and m-tolunitrile. Two photochromic dyes shown in the study to be compatible with these dielectric fluids are spiropyran and triarylmethane.

These combinations of dielectric fluids and photochromic dyes should be adequate to produce baroclinic instabilities using radial electric potentials of less than 15 kilovolts across a nominal 1 centimeter gap. The dot matrix generated by the dye following its exposure to UV light should last for more than sixty seconds thereby allowing time for observations of the fluid flow dynamics.

An important aspect to the successful use of these fluids lies in the details of the purification process necessary to achieve a low dissipation factor of 0.002 to minimize fluid heating by the electric field. The implementation of an adequate purification process was beyond the scope of the present study. The procedure for its development was defined, however. Available data on these fluids, although sparse, do indicate that acceptable properties are feasible when sufficient care is taken during purification and handling.

The material for the outer sphere of the flow cell was selected to be sapphire because of its optical transparency and good thermal conductivity for control of thermal gradients. Solid hemispheres with radii up to 4 centimeters are available with their optical axis within 5 degrees of the axis of rotation for

the experiment. Hemispheres with radii up to 7.5 centimeters can be manufactured with their optical axis orthogonal to the axis of rotation. In either case, the effects of birefringence from the sapphire must be accommodated by the experiment either during data collection by polarization or data processing by calibration of the predictable but changing optical effects on the detected thermal gradients.

The inner sphere of the flow cell serves as a specular reflector for the data collection system as well as the active thermal control for the experiment. A combination of electric heaters placed 10 degrees apart on a meridional arc and thermoelectric modules (for cooling and heating) located at the equator and pole are used to establish the linear thermal gradients for the experiment. Using available calculations of fluid flow dynamics, a thermal analysis was performed using an explicit 53 node model to establish the performance requirements for the sphere's heaters and coolers. The largest cooling load is 9.5 watts on the inner sphere while the largest heating load is 16 watts on the outer sphere. Within this operating range, all thermal cases of interest can be accommodated. Heat exchange with the external environment is accomplished by gas flow within the experiment assembly and energy exchange by co-rotating conductive fins. It is estimated that 57 kilograms per hour of avionics air supplied by the Spacelab will be sufficient to handle the 277 watt thermal load generated by the flow cell and its associated equipment (i.e. power supply, electronics, heaters, coolers, fan, etc.).

The driving force for the circulation experiment is the radial electric field simulating the gravitational force of earth. The dominant parameters controlling the magnitude of the force are the dielectric constant for the fluid and the magnitude of the applied voltage. A judicious choice for the combination of

these two parameters can ease their implementation difficulties. The study results indicate that fluids with dielectric constants between 5 and 40 can be used satisfactorily with voltages less than 15 kilovolts. A 15 kilovolt power supply (HVPS) was designed using a series resonant circuit to meet the experiment requirements for control, stability and linearity while operating at a 300 Hz frequency. The HVPS, as shown in Figure 1.1-3, fits on the rotating experiment table adjacent to the flow cell assembly.

Operation at 300 Hz has been selected to minimize the motion by particles trapped within the fluid. An on-line filtering system has been incorporated into the AGCE to minimize their population. Any residual particles escaping the filtering system can disrupt through interaction with the electric field the observation of the flow effects being sought in the experiment. It has been observed however that operation at or above 300 Hz for the electric field minimizes the motion that can be imparted to a particle before the field reversed direction. The combination of filtering and AC fields will reduce perturbations from stray particles.

The observation of the circulation effects relies on the generation of time-sequential maps of both fluid circulation and thermal gradients over substantially a full hemisphere of the rotating test cell that models the earth's atmosphere. This study has shown that the measurement requirements of the AGCE can be met by a relatively simple instrument using a flying-spot scanner. A preliminary design has been shown capable of surveying one hemisphere of the rotating test cell at a 1 degree resolution over a 69 degree span of latitude. This scanner can observe and measure the two non-radial components of thermal gradient in the test fluid with 0.01 degree C/cm resolution at a signal-to-noise ratio (SNR) of at least 6. Photochromic marker dots can be observed

simultaneously with a SNR in the hundreds. The same detectors can also feed a closed circuit television (CCTV) display for the payload specialist, with a SNR in the hundreds.

The flying-spot scanner is based on the monocentric (Offner) relay. The optical path has been folded away from the test cell itself, to avoid physical interference. The folding mirror (or mirrors) has been chosen to be semi-reflective because it maximizes the scan angle and allows the scanning beam to pass through the test fluid almost radially. This is important for minimizing the volume of fluid intercepted by the scanning beam and therefore maximizing the spatial resolution of the instrument. The monocentric relay is implemented using a solid glass design assembly because it results in a smaller and more stable instrument, is easier to realize the semi-reflective folding mirror as a buried-surface beamsplitter, and fresnel losses can be better controlled. The solid Offner relay has been designed to be achromatic over the normal visible spectrum. The nominal relay design has been based on the mid-image height (3.30 mm) and the sodium D-line (5893 angstroms).

The rapid rotation rate (10,300 RMP) on the scanner head which is necessary to handle the cell rotating at its maximum rate of 3 rad/sec makes it impractical to attempt putting electrical power in or out of the head while in motion. The detector therefore can not be physically mounted on the scanner head. The solution selected is to use again Offner relays to put images of source and detector onto the scanner head. The scanner head incorporates a fully reflective buried folding mirror that will rotate these images into the self-conjugate plane. There they will function exactly as would physical sources and detectors. The only part that moves, now, is the small glass scanner head, which should be made symmetrical for dynamic balance. Detectors considered for the allowed

detector configuration include the following: UPT PIN Spot/2D and Hughes HPIN 100D, which are both available as chips. The basic design constraint is the chip size to accommodate the image height at the center of 3.30 mm and fit physically close to each other in a four quadrant arrangement.

The baseline design was analyzed to ascertain whether the image quality was satisfactory and whether the sensitivities to thermal gradient and marker dot opacity are consistent with design goals. The image quality was assessed using ray tracing computational methods. Instrumental sensitivity was determined by photometric analysis. The design has been shown through ray tracing to exhibit outstanding image quality and to yield a signal that is linear with thermal gradient over at least two decades of dynamic range.

The flying-spot scanner instrument being fundamentally simple in design should be realizable at modest cost. Volume and weight will be small in comparison with the rest of the experimental apparatus.

The type and quantity of data to be generated by the AGCE played a key role in the selection of the philosophy for experiment control and data handling. The AGCE data, unlike that for the GFFC, are in electronic form and being generated at a relatively high rate. In a trade-off study between on-board electronic video recording and telemetry, telemetry was judged to be the better approach because it produced a simpler, less costly flight package and allowed for a more direct role on the part of the principal investigator (PI) during the course of the flight.

On-board recording not only requires a video recorder and interfacing circuitry but also suitable displays and controls for the payload specialist (PS) to assess and control performance. In flight form, this equipment adds

subetantially to the cost of the flight system and minimizes PI involvement. In contrast, telemetry of experiment data to the Payload Operation Control Center (POCC) permits a shift in roles of the PI and PS such that the PI directly assesses and indirectly, via the PS, controls system operation. Thus the telemetry mode does not require on-board displays; rather these displays reside in the AGCE Ground Support Equipment (GSE) which can be used also in qualification and acceptance testing as well as for PI use at the POCC.

This overall experiment control and data handling philosophy is particularly well-suited to the nature of the implementation scheme selected for the AGCE. The approach not only lowers the cost of the flight unit but maximizes the use of the GSE and provides a high level of direct interaction by the principal investigator which is a necessary ingredient in the conduction of a scientific experiment.

The feasibility study for the Atmospheric General Circulation Experiment (AGCE) examined all of the technical areas critical to the successful implementation of the experiment on Spacelab. The overall conclusion to be drawn from the study results is that the AGCE is feasible for Spacelab with no identifiable technical obstacle to block its successful completion. Furthermore, the flexibility in the design parameters for the AGCE should be sufficient to permit good sensitivity in exploring the onset of baroclinic instabilities for terrestrial atmospheres. Sufficient variability exists in design parameters such as fluid dielectric constant, sphere cell diameter, experiment cell gap, range of thermal control and applied high voltage to allow considerable flexibility in establishing the experiment parameters. This flexibility can contribute significantly to adequately mapping conditions controlling baroclinic instabilities. The flexibility is further increased by the ability of the principal investigator to

receive, evaluate and react in real-time to the AGCE results. This ability for the PI is achieved by the experiment control and data handling procedures selected for the AGCE.

The configuration for the AGCE fits well within a single experiment bay rack and can effectively mate with the services required for its operation.

The recommendations to be made lie principally in the realm of technical activities to insure a sound design with good performance margin. The recommendations of most significance are:

a) it is highly recommended that the fluid purification and characterization program outlined in this study be completed early in the AGCE final hardware design effort;

b) it is highly recommended that a general tolerance and sensitivity analysis for the system be done to establish limits on performance expectation and provide a basis for cost effective allocation of fabrication tolerances;

c) it is recommended that polarization of light in the optical scanner system be given further attention for data processing to accommodate birefringence and rotation affects;

d) it is recommended that further investigation be given to the selection and verification of heat transfer properties of materials; this is most significant to achieving the predicted thermal control capability;

2.0 RESULTS OF THE AGCE FEASIBILITY STUDY

2.1 BACKGROUND

An Atmospheric General Circulation Experiment (AGCE), which will model the large-scale circulations of the earth's atmosphere in hemispherical geometry, has been proposed for Spacelab flights. In this experiment the working fluid will be held between two concentric spheres and subjected to a radial electric field in the form of a spherical capacitor. The pole-equator temperature gradient and the large-scale vertical stability of the atmosphere will be modeled by maintaining latitudinal temperature gradients on the spheres and by maintaining the outer sphere warmer than the inner sphere. The rotation of the earth will be modeled by co-rotating the spheres.

Much sophisticated laboratory modeling of the effects of rotation and differential heating on fluids has previously been carried out in cylindrical geometries, and much has been learned which is relevant to the general circulation of the earth's atmosphere. However, these models have serious limitations when attempts are made to extend their results to the spherical geometry of the atmosphere. The principal objectives of the AGCE system are to examine (in the spherical model) the onset of the wave-cyclone (baroclinic) instability, the growth rates and length scales of this instability, and the stationary and time-dependent finite amplitude flows achieved as a consequence of the instability.

Scientific theoretical design studies for the AGCE have shown that it will not be easy to construct an apparatus in which the required baroclinic instability can be realized. A fluid with a high dielectric constant, low dissipation factor, low viscosity and other specific properties is required. A relatively

large AC voltage is required. It has been found that dust particles in the fluid are agitated by the electric field and can in turn stir up the fluid. These dust particles must be removed. Observation of the flow over a latitudinal range of 90^{o} is desired. Further, the observational and thermal requirements imply that the outer sphere must be transparent and a good thermal conductor. It remained at the start of the study to determine if a suitable material of the required dimensions could be made. It is the intent of this AGCE feasibility study to examine these concerns before proceeding to an engineering flight hardware design and fabrication contract.

Hardware for a similar spherical geophysical fluid dynamic experiment is currently under development for NASA by the Aerojet General Corporation. This experiment, the Geophysical Fluid Flow Cell (GFFC), is concerned with modeling convectively unstable circulations as are found in stars. In the GFFC the inner sphere will always be maintained at a higher temperature than the outer sphere.

Although the science in general and the fluid dynamic capabilities in particular of the GFFC experiment and the AGCE are essentially different, the engineering and the hardware for both experiments have much in common. Thus wherever possible, the GFFC design experience was used to guide the AGCE system design.

Table 2.1-1 lists the specific tasks identified by the contract work statement which were accomplished during the AGCE feasibility study effort. Note that it was not the intent of the feasibility study to generate detailed flight hardware designs but rather to accomplish sufficient analyses and preliminary designs to establish feasibility of the AGCE system as a Spacelab experiment. The following sections have grouped the tasks into common technical areas wherever possible.

The results of the feasibility study are summarized in Section 2.0 contained in

Volume I. The documentation generated during the course of the study which contributed to the results are included in Section 3.0 contained in Volume II.

Table 2.1-1

Specific Tasks Accomplished During the AGCE Feasibility Study

Task	Scope
Task 1 - Survey of Dielectric Fluids	Performed survey to identify suitable high dielectric fluids compatible with photochromic dye materials.
Task 2 - High Voltage/ High Frequency Source	Performed study to determine feasibility of equipment to generate high voltages (up to 20-30 kV RMS) over a frequency range of 60 to 1000 Hz.
Task 3 - Dust Removal	Performed design study on the feasibility of incorporating a hardware capability for programmed circulation and filtration of the dielectric fluid after system assembly.
Task 4/5 - Flow/Thermal Gradient Observation	Performed design study to determine feasibility of using a flying spot scanner technique for monitoring and recording thermal gradients and fluid flow, i.e. thermal and flow mapping, in the dielectric fluid from pole to equator.
Task 6 - Thermal	Performed heat flow calculations and determined the feasibility of maintaining the desired flow cell sphere temperature distribution.
Task 7 - Control	Performed study to determine feasibility of data handling and system control compatible with results of Tasks 1 thru 6.
Task 8 - Material	Determined availability of suitable material for the outer sphere of the flow cell.
Task 9 - Configuration	Determined feasibility of AGCE flight configuration and assessed feasibility of flow cell interchangeability.
Task 10 - Cost Estimate	Using the RCA PRICE cost models, generated a cost estimate for designing and fabricating one AGCE flight system.

2.2 MATERIALS FOR DIELECTRIC FLUID AND EXPERIMENT SPHERE

2.2.1 Survey of Dielectric Fluids

The AGCE Statment of Work (SOW) listed several characteristics which the "ideal" dielectric fluid should possess. Most of the values listed were for the Dow Corning 200 oil used in the GFFC with the exception of the dielectric constant for which a factor of 20 increase is desired. The key parameters identified in the SOW and the desired values are given below.

1) Dielectric Constant: >40 ε_o. However, any value greater than 2.2 ε_o will be helpful (ε_o = dielectric constant of free space = 8.85×10^{-12} farad/meter).
2) Dissipation Factor: 4×10^{-5} in the frequency range around 500 Hz. The heating rate should not exceed $0.001^{o}C$/sec.
3) Electric Volume Resistance: 1×10^{14} ohm/cm. A lower value might be satisfactory to maintain the heating rate below $0.001^{o}C$/sec.
4) Dielectric Strength: >50 volts/mil. The required value will depend on the sphere separation and voltage level. For the nominal values of 20 kV and 1 cm separation, a rating of approximately 51 volts/mil would be required at 1 cm. Translating this requirement to the standard rating, usually measured for a separation of 0.1 inch, yields a value of approximately 102 volts/mil (dielectric strength is inversely proportional to square root of dielectric thickness).
5) Viscosity: <5 centipoise. Preferably <1 centipoise. The upper limit was later fixed at 3 cp (PIR No. 1254-AGCE-009 in Section 3.1, Volume II).
6) Coefficient of Volume Expansion: $>1 \times 10^{-4}\ {}^{o}C^{-1}$.

7) Transparency: Clear or almost clear. In addition, the fluid must be compatible with a photochromic dye to permit implementation of the flow visualization technique.

Since discussions with experts in the field of dielectric fluids indicated that items (4) and (6) could be satisfied by a large number of fluids these areas were not emphasized in the survey. The requirements on dissipation factors and electric volume resistivity (items 2 and 3) were combined into a consideration of dissipation factor only, since it is the more accurately measured parameter and includes all effects which contribute to fluid heating (including resistivity).

As the study progressed, the importance of fluid purification on the achievable dissipation factor (and resulting fluid heating) became apparent and an additional effort was devoted to that area. Thus, the results of the survey of dielectric fluids are divided into three major areas: (1) fluid characteristics assessment, (2) fluid purification, characterization and handling, and (3) fluid/photochromic compatibility assessment. An additional output of the study is a definition of areas which were beyond the present scope but require consideration before a hardware development program is initiated.

2.2.1.1 Fluid Characteristics Assessment

Three fluid characteristics critical to the successful performance of the AGCE are the dielectric constant, viscosity and dissipation factor. Since the Statement of Work emphasized the need for high dielectric constants, the initial study effort addressed the variation of viscosity and dissipation factor as a function of dielectric constant.

A table of solvents for chromatography (Kodak Publication No. JJ-3) was used as the basis for this assessment. A representative selection of fluids from that listing is given in Table 2.2-1 with values for the dielectrical constant (K), and the viscosity (μ). The essentially random variation of viscosity as a function of dielectric constant is clearly indicated in Figure 2.2-1.

Selecting a fluid with viscosity acceptable to the AGCE should not be a problem. More than 80% of the fluids in Table 2.2-1 have viscosities less than the required upper limit of 3 cp and over 50% have values below the desired upper limit of 1 cp. Three fluids known to be compatible with photochromics (see below) are identified in Figure 2.2-1.

Similar attempts to quantify the dissipation factor as a function of dielectric constant were unsuccessful due to a paucity of data on dissipation factors for fluids of high dielectric constant. Subsequent information obtained through discussions with personnel at the National Bureau of Standards, Monsanto, Crown-Zellerbach and the GE Capacitor Products Department indicated that the dissipation factors of high dielectric constant fluids are extremely difficult to measure and the values obtained are highly dependent on the fluid purity (hence the scarcity of tabulated data).

In lieu of data permitting an exact quantification of the achievable fluid dissipation factors, a parametric analysis was performed to establish the interrelationship between the dissipation factor, dielectric constant and heating rate of the fluid and the experiment operating voltage The results are given in Figure 2.2-2 for the nominal AGCE design configuration of

r_i = 5.0 cm (outer radius of inner sphere)

r_o = 6.0 cm (inner radius of outer sphere)

f = 300 Hz (frequency of applied voltage)

Table 2.2-1

Representative List of Solvents Commonly Used in Chromatography with Values of Dielectric Constant and Viscosity

Chemical	Dielectric Constant K	Viscosity μ
Pentane	1.80	0.240
Hexanes, Reagent ACS	1.89	0.326
Cyclohexane, Reagent ACS	2.02	1.020
Cyclohexene	2.22	0.660
Carbon Tetrachloride, Reagent ACS	2.24	0.969
Benzene, Reagent ACS	2.30	0.652
m-Xylene	2.37	0.620
Toluene, Reagent ACS	2.38	0.590
Ethylbenzene	2.41	0.691
x-Xylene	2.57	0.810
Propyl Ether	3.40	0.378
Bromoform	4.39	2.152
Chloroform, Reagent ACS	4.81	0.580
Butyl Acetate	5.01	0.732
Bromobenzene	5.40	1.196
Chlorobenzene	5.90	0.799
Ethyl Acetate, Reagent ACS	6.02	0.455
Acetic Acid, Glacial, Reagent ACS	6.15	1.300
Methyl Acetate	6.68	0.381
Aniline, Reagent ACS	6.89	4.400
Ethyl Formate ACS (Pract.)	7.10	0.402
1,1,1-Trichloroethane (Techn.)	7.52	1.200
Octyl Alcohol	10.34	10.600
m-Cresol (Pract.)	11.80	20.800
Pyridine, Reagent ACS	12.30	0.974
Benzyl Alcohol	13.10	5.800
Butyl Alcohol, Reagent ACS	17.10	2.948
Isobutyl Alcohol, Reagent ACS	17.70	4.703
Isoprophyl Alcohol, Reagent ACS	18.30	2.320
Prphyl Alcohol	20.10	2.256
Acetone, Reagent ACS	20.70	0.316
Acetaldehyde	21.10	0.220
m-Nitrotoluene	23.00	2.330
Benzonitrile, Spectro Grade	25.20	1.240
o-Nitrotoluene	27.40	2.370
Methanol, Reagent ACS	32.80	0.597
Nitrobenzene, Reagent ACS	36.10	2.030
Acetonitrile, Reagent ACS	37.50	0.345
Ethylene Glycol	37.70	19.900
Nitromethane, Spectro Grade	39.40	0.620
Formic Acid, Reagent ACS	47.90	1.804
Formamide, Reagent ACS	109.50	3.300

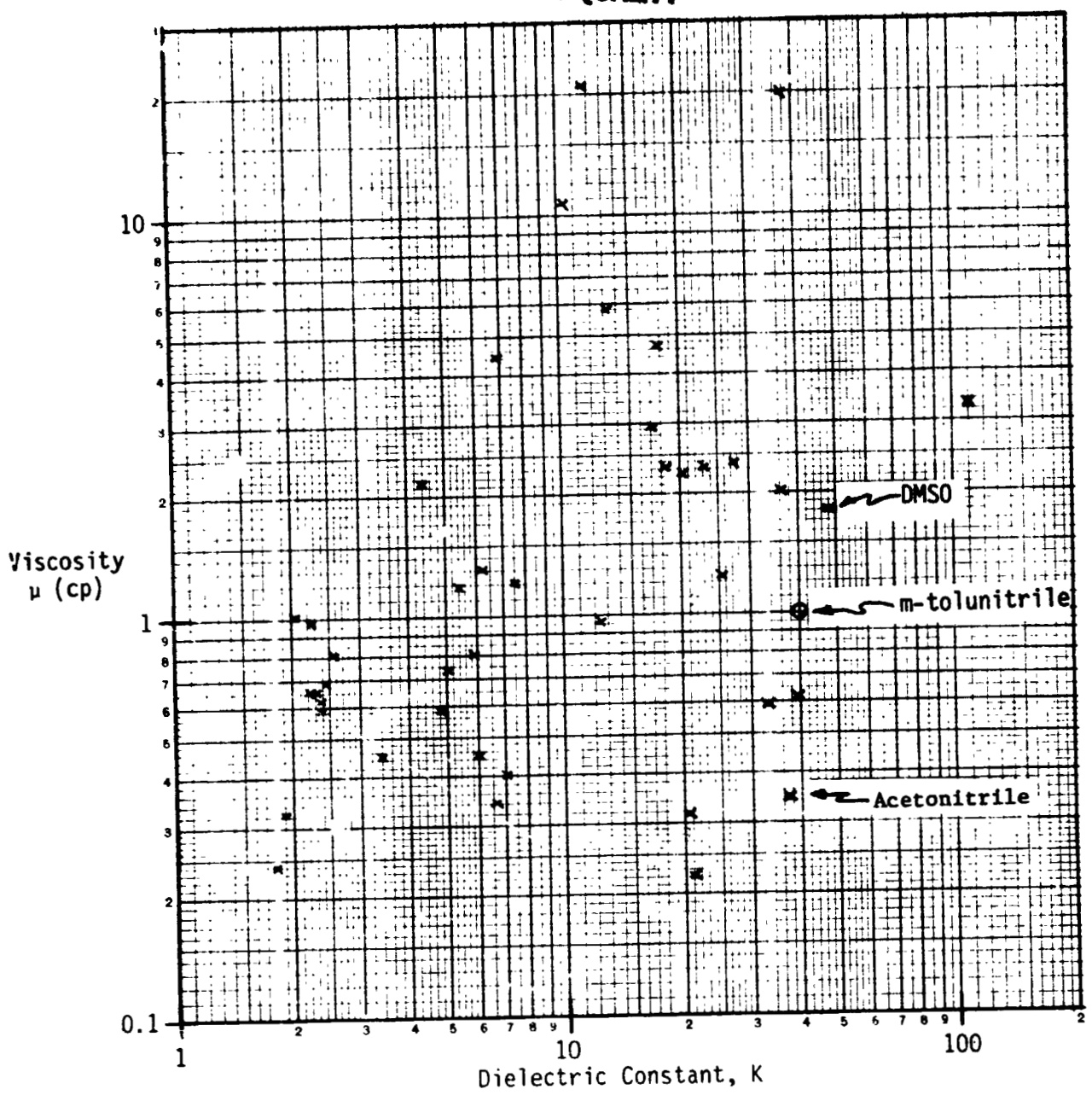

Figure 2.2-1. Illustration of variation in fluid viscosity for fluids of increasing dielectric constant.

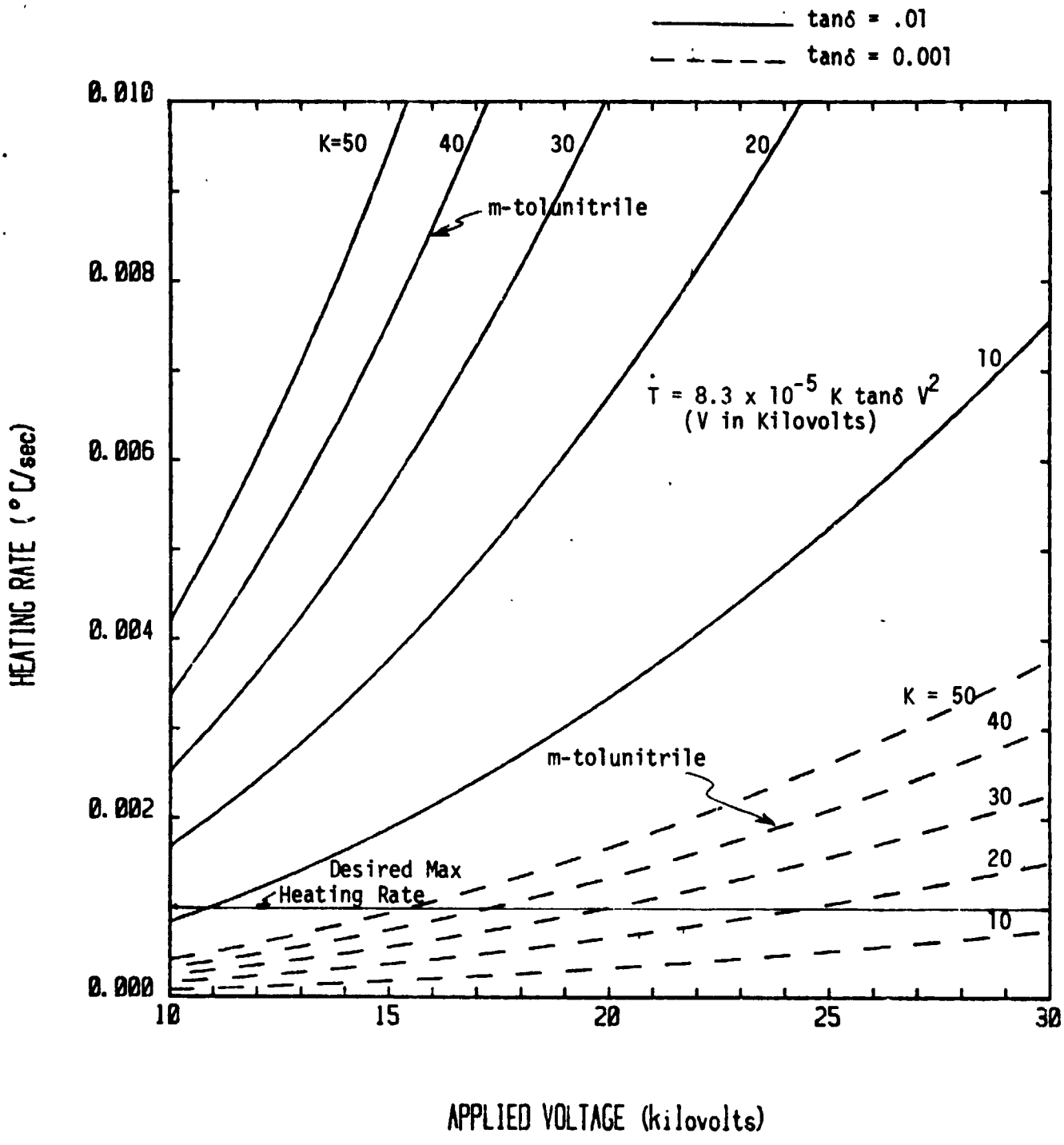

Figure 2.2-2. Fluid Heating Rate as a Function of Applied Voltage for Selected Values of Dielectric Constant (K) and Dissipation Factor (tanδ).

As shown, for an operating voltage of 15 kV and a fluid dielectric constant of 40, a dissipation factor of ∿0.002 is required to remain below the desired maximum heating rate of 0.001°C/sec. Obtaining a high dielectric constant fluid of sufficient purity to achieve this low dissipation and then maintain the purity is very difficult. A suggested fluid purification procedure for the AGCE is discussed below.

2.2.1.2 Fluid Purification, Characteristics and Handling

A procedure for evaluating fluids for use in the AGCE was outlined based on personal communication with experts in the area of fluid purification and evaluation, and a review of pertinent published papers. These sources all indicated that special facilities were required to accurately measure electrical properties such as dielectric constant and dissipation factor of high dielectric fluids. When highly purified fluids are required it is almost essential that the purification and characterization be performed in the same laboratory. At present only the GE Capacitor Products Department appears to have this combined capability. The following general steps were identified as the best AGCE fluid purification procedure.

1) Fluid filtration using membrane or depth type filters to remove non-colloidal solid particulates (>0.1 micron).
2) Dehydration and deaeration using a combination molecular sieve and vacuum treatment to remove dissolved water and gases.
3) Final purification using an adsorbent such as fuller's earth to remove colloidal solids (<0.1 micron), molecules and ions.

The specifics of implementing each of these steps can vary depending on fluid characteristics such as viscosity, density and dielectric constant, and in some cases the procedures are proprietary. For example, although the Monsanto

Chemical Company and Crown-Zellerbach have what they consider to be good purification procedures, neither would divulge any details of their processes.

Candidate fluids chosen for the AGCE application must be characterized to establish their electrical parameters and to assess their contamination potential. Electrical property measurements should be made at several points in the purification process to establish the effectiveness of each step and to determine the optimum purity achievable, i.e., the point at which further processing is of no value.

Assessment of contamination potential requires that the same set of fluid property measurements be made periodically after the purification is completed. During this post purification time, the fluid must be placed in contact with candidate materials to be used in the AGCE fluid system and exposed to various light sources. The photochromic dye must also be mixed with the purified fluid and its effects on the fluid properties assessed. Periodic measurements must also be made on a control sample of the purified fluid which is maintained in a dark place in a non-reactive container. These measurements will allow the effects of various materials to be compared with fluid degradation due to the normal aging process.

A logical conclusion of the stringent fluid purification and characterization procedure is that all fluid handling procedures must be minimized. The recommended handling procedure for storage and/or transfer of the fluid from the purification apparatus to the AGCE assembly will be based on the results of the fluid characterization (i.e., contamination susceptibility). The major environmental parameters which are likely to require special consideration during the transfer process are (1) exposure to air, (2) contact materials, and (3) exposure to light.

As previously mentioned, the difficulties associated with the purification and characterization of high dielectric fluids has resulted in a paucity of data for fluids of interest to the AGCE application. Although scattered data are available for a few fluids, the values depend strongly on the fluid purity and the measurement techniques, making it difficult to establish trends. The results presented in Table 2.2-2 should be interpreted as indicative of what may be feasible in terms of dissipation factor and/or resistivity.

2.2.1.3 Fluid/Photochromic Compatibility

Laboratory tests were conducted at both the General Electric Space Systems Division and at the Rochester Institute of Technology (RIT) to assess the compatibility of several solvents and photochromic dyes. The detailed results are documented in PIR Nos. 1254-AGCE-025, 032, 036, and 037 found in Section 3.1 of Volume II, Detailed Feasibility Study.

The response properties for relevant photochromic dye-solvent systems as measured by Dr. Francis of RIT are given in Table 2.2-3. The density of the solutions were measured at 625 nm (as the dyes tested yield solutions which are cyan and green in color). The density values given are to be considered to be only relative numbers, for intercomparing the solutions only.

With regard to obtaining density, there is no difficulty in dissolving either dye in any solvent tested thus far. (Mild heating to 80°C for a few minutes was required in the case of ethylene glycol.) The dye concentrations used were 1 mg/cc of solvent. The saturation point of dye in solvent does not appear to have been even closely approached in these solutions. More dye dissolved in the solutions will result in more density, but linear increases with concentration are not expected, since dye solutions show departures from Beer's law behavior.

Table 2.2-2

Data for a Range of Dielectric Fluids

FLUID (DIELECTRIC CONSTANT)	PURIFICATION PROCESS	LABORATORY	DISSIPATION FACTOR (RESISTIVITY)	COMMENTS
*m-tolunitrile (40)	Molecular Sieve & Fuller's Earth	GE Capacitor Products Department	<0.01	A tan δ of ≈0.001 may be achievable.
*DMSO (∿48)	Proprietary	Crown Zellerbach	($\sim 10^{8}$ Ω cm)	
Aroclor 1242 (5)	Proprietary	Monsanto Company	∿0.0015	Very viscous
MCS 1489 (6.5)	Proprietary	Monsanto Company	0.05	Developed as a substitute for Aroclor fluids
Nitrobenzene (∿35)	Not specified	NBS	(6.67×10^{8} Ωcm)	This sample probably was not highly purified
Nitrobenzene (∿35)	Fractional Distillation & Freezing followed by Electrodialysis	--------	(7.5×10^{13} Ωcm)	This value was reported in a paper by Pearmain, et al.

*These fluids are known to be compatible with photochromic dye material.

Table 2.2-3

Response Characteristics for Relevant Photochromic Dye-Solvent Systems Measured by Dr. Francis at RIT

Dye	Solvent	Dielectric Constant	D_{625}	$Fade_{1/2}$ (sec)
BMS	DMSO	47.0	0.12	27
BMS	Eth. Glycol	38.0	0.02	78
BMS	2(2-ethoxy)		0.31	9
BMS	MEOH	33.0	0.05	19
BMS	TN	40.0	1.2	5
BMS	Cyclohexanone	18.3	~0.9	5
BMS	Chloroform	4.8	~0.9	9
MGCN	DMSO	47.0	0.89	110
MGCN	2(2-ethoxy)		1.30	~3600
MGCN	DMF	38.0	0.6	25
MGCN	AN	38.0	0.6	See text

BMS = 5'-bromo-8'-methoxy-6'-nitro-1-phenyl-3,3-dimethyl-indolinobenzopyrylospiran

MGCN = malachite green leuco cyanide

DMSO = dimethysulfoxide

Eth. glycol = ethylene glycol

2(2-ethoxy) = 2(2-ethoxyethoxy) ethanol

MEOH = methylalcohol

TN = m-tolunitrile

DMF = dimethylformamide

AN = acetonitrile

D_{625} = density of the exposed solution at 625 nm

$Fade_{1/2}$ = time for exposed solution to lose one-half the maximum density obtained upon exposure

The colored form of the dye will also absorb actinic radiation that could otherwise be used to activate as yet uncolored dye molecules in the solution. This phenomenon is known as "internal filtering". Increased densities are also expected with radiant sources of greater output at actinic wavelengths.

Relative densities up to 1.30 have been produced with $fade_{1/2}$ times up to 3,600 seconds. In the case of the MGCN, the fade times can be adjusted to shorter times by small concentrations of sodium cyanide added to the solutions, a control not available in most photochromic dye systems. Sodium cyanide is freely soluble in dimethylsulfoxide and 2(2-ethoxyethoxy) ethanol. It is to be anticipated that this will be accompanied by some loss of density.

The solvent 2(2-ethoxyethoxy) ethanol has been found to give the highest densities thus far for both BMS and MGCN dye. The dielectric constant for this solvent has not been found, but the results are included as it is conceivable that it is in the range of interest since this solvent is in the alcohol class of compounds. However, its high viscosity of approximately 3.8 cp makes it unacceptable for AGCE applications.

Malachite green leucocyanide in acetonitrile requires a special note. In previously unpublished work by Dr. Francis, it has been noted that, in the case of some triarylmethane photochromic-solvent pairs, carbon dioxide, oxygen or water from the air influence reponse. One result is the continued increase in density after exposure is terminated and very long fade times. Precipitations have been noted. A spontaneous switching of the solution from the colored to colorless state, repeating many times can also be observed. The nature of these complex solutions has not been completely elucidated.

Malachite green leucocyanide in acetonitrile represents one such case, and while

exposure produces significant density, the complex behavior described above lessens the attractiveness of this system. The solution eventually fades, and stirring of the solution diminishes the effect of any long-fade time density. The malachite green leucocyanide-acetonitrile system can be returned to normal fading behavior immediately upon termination of exposure if the acetonitrile is purged with nitrogen (approx. 4 minutes for 10 ml of acetonitrile). Air must be scrupulously excluded subsequently. Since the AGCE will provide a closed system, which illiminates exposure of the fluids to air, the above complications may not be a problem in the operational system.

This behavior is not observed with all triarylmethane-solvent pairs and it has not been observed in any case with the spiropyrans.

Limited fatigue studies have been performed by cycling solutions through expose and fade for as many as twenty times. Fatigue is the property of photochromic solutions whereby their optical properties change upon repeated cycling. The photochromic solution may show less density with repeated exposure; it may fade more slowly, or it may take on a permanent color. However, fatigue should not be a problem for the AGCE since only a very small percentage of the fluid is activated for each measurement. Subsequent mixing of the fluid makes it unlikely that the same parcel of fluid will be activated several times.

Qualitative laboratory tests were also performed at GE to assess several photochromic dye/fluid combinations in terms of (1) the solubility of the dye, (2) the response of the solution to exposure to UV light, and (3) the fade time of the solution. Two combinations which exhibited behavior consistent with the requirements of the AGCE were a spiropyran photochromic dissolved in m-tolunitrile and a triarylmethane photochromic dissolved in dimethylsulfoxide (DMSO). Both solutions darkened when exposed to UV light and returned to their

original, nearly transparent states within a few minutes. The compatibility of the triarylmethane/DMSO combination was also verified by Dr. Francis of the Rochester Institute of Technology (see above).

Transmission curves for these two solutions are given in Figures 2.2-3 and 2.2-5. As shown, although the maximum absorption regions of the two solutions differ slightly, both combinations are capable of reducing the transmittance by up to 75%. If the fade time (τ) is defined as a function of transmittance by Equation (1)

$$\tau = t\left[T_o + \frac{(T_F - T_o)}{2}\right] \qquad (1)$$

where T_o and T_F are the initial (t=0) and final transmittances, then from Figures 2.2-4 and 2.2-6 fade times of approximately 110 sec and 70 sec are calculated for the m-tolunitrile and DMSO solutions, respectively. Therefore, both solutions appear acceptable from the standpoint of fade time and transmittance change when activated.

Although hardly any photochromic compounds are commercially available, Dr. Francis has considerable experience in the preparation of spiropyran and triarylmethane compounds. Procedures are known for the preparation of a wide variety of these two classes of compounds and it should be possible to prepare a variety of them, in quantities sufficient for the AGCE, without any experimental difficulty. The synthesis of the spiropyrans generally require a number of procedural steps, and the preparation of specific compounds can be time consuming. One such compound for example required 80 hours to prepare. The triarylmethanes are generally simpler to obtain.

The known characteristics of photochromic compatible fluids which have been investigated to date are summarized in Table 2.2-4.

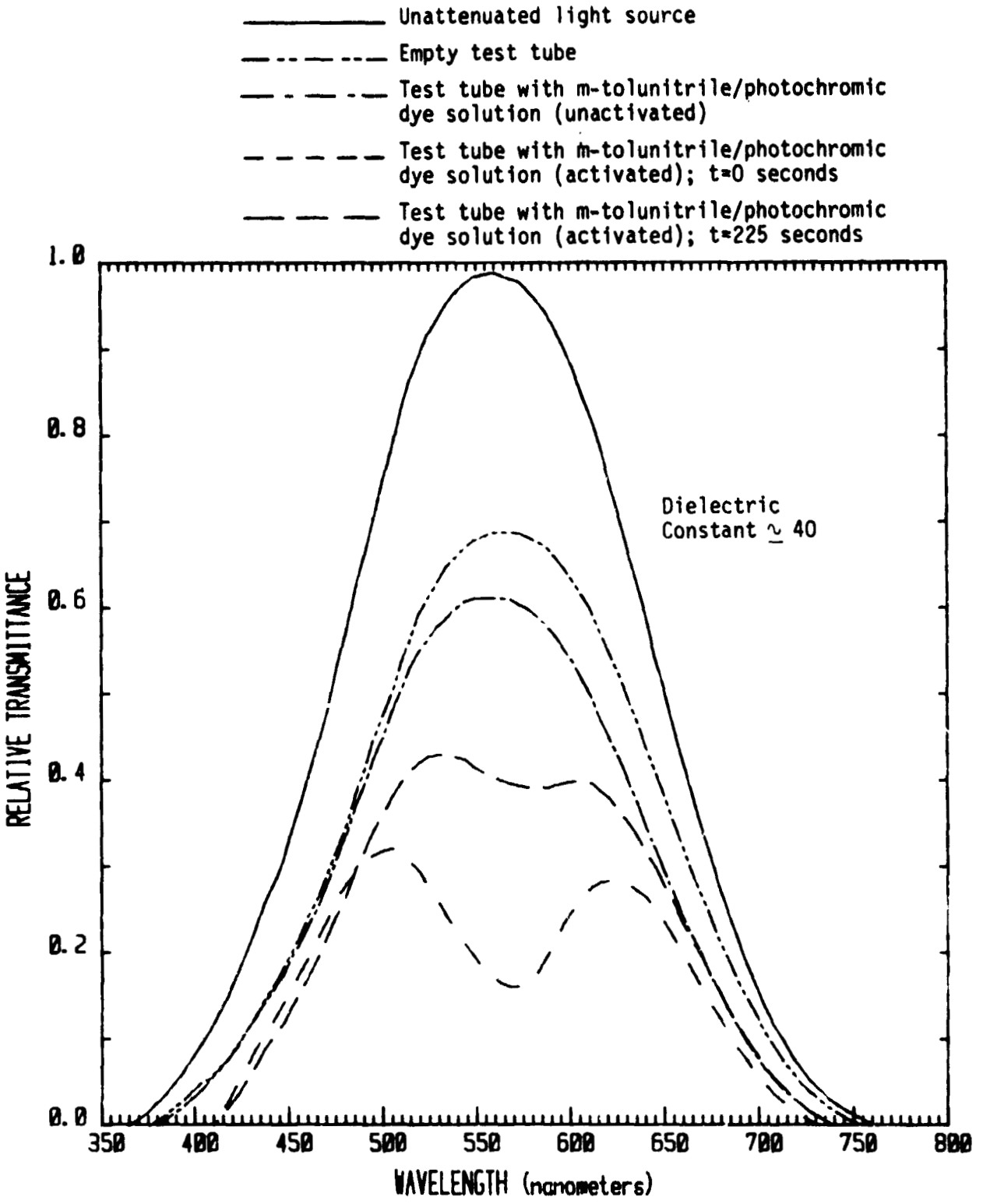

Relative transmittance of m-tolunitrile with a photochromic dye (spiropyran, TNSB) in solution. Transmittance curves in the activated state were obtained immediately after and ~ 225 seconds after activation.

Figure 2.2-3

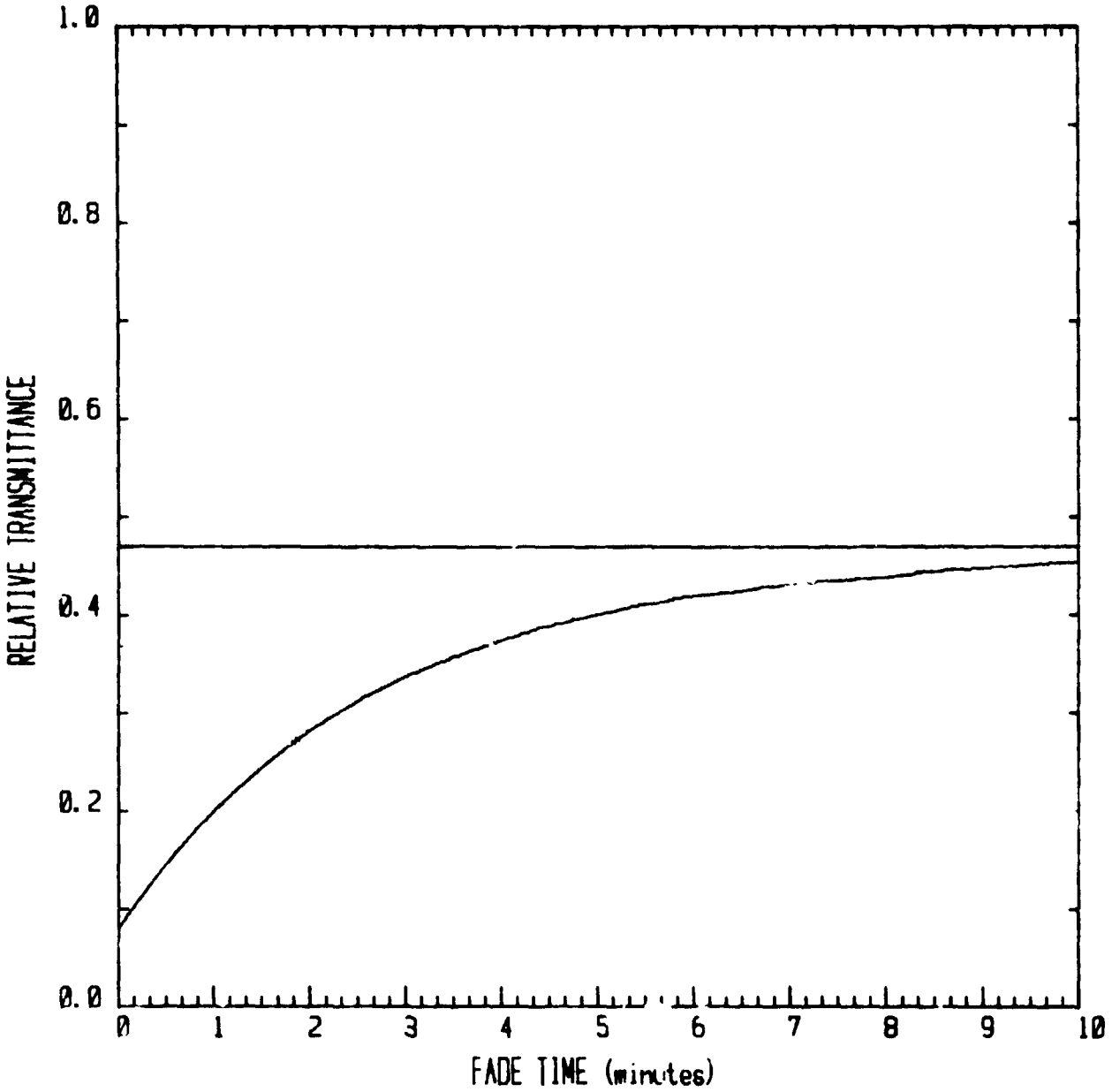

Fade time for a solution of m-tolunitrile and a spiropyran class of photochromic dye (TNSB). Transmittance measured at ∿560 nm.

Figure 2.2-4

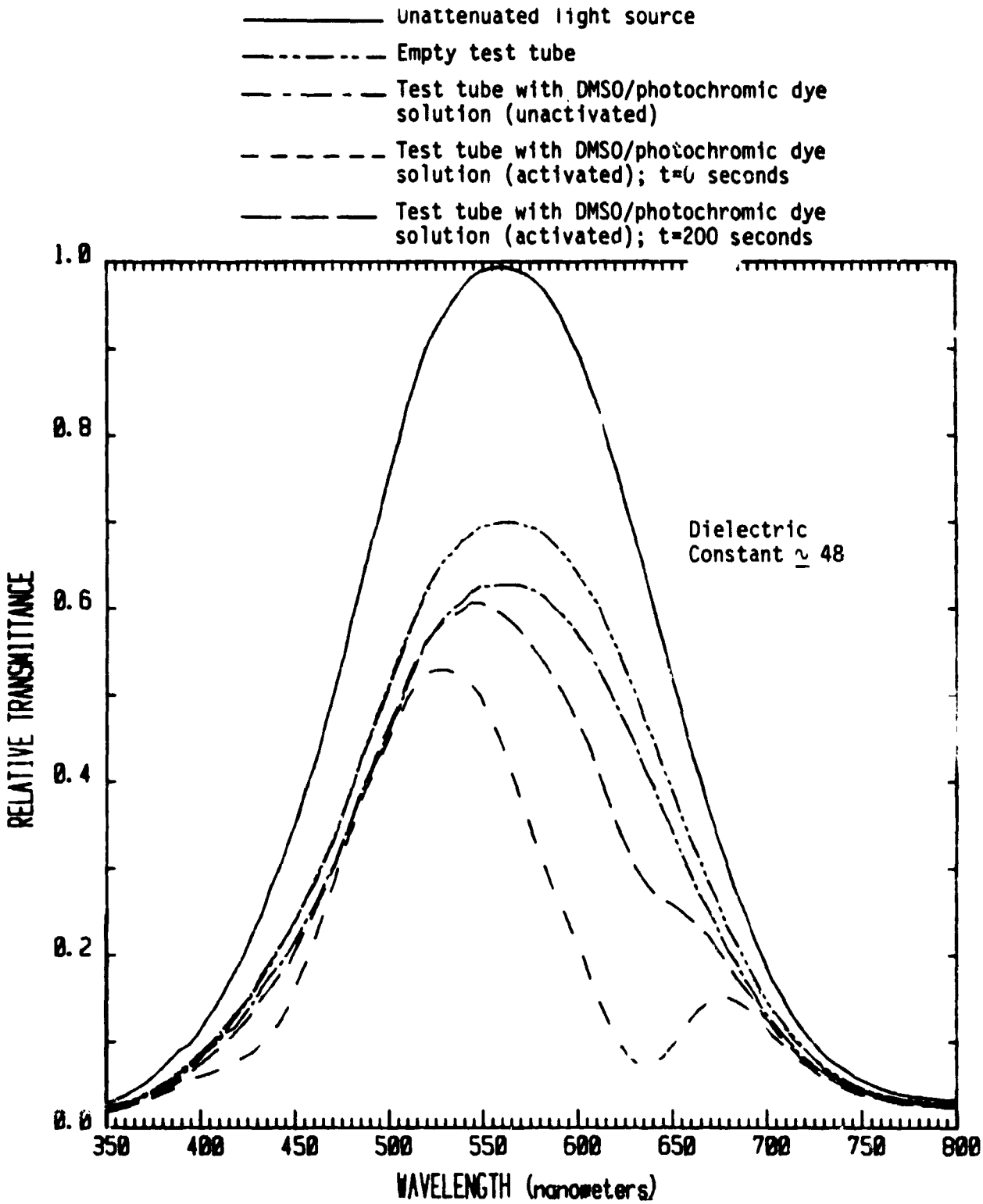

Relative transmittance of DMSO with a photochromic dye (triarylmethane, malachite green leucocyanide) in solution. Transmittance curves in the activated state were obtained immediately after and ~ 200 seconds after activation.

Figure 2.2-5

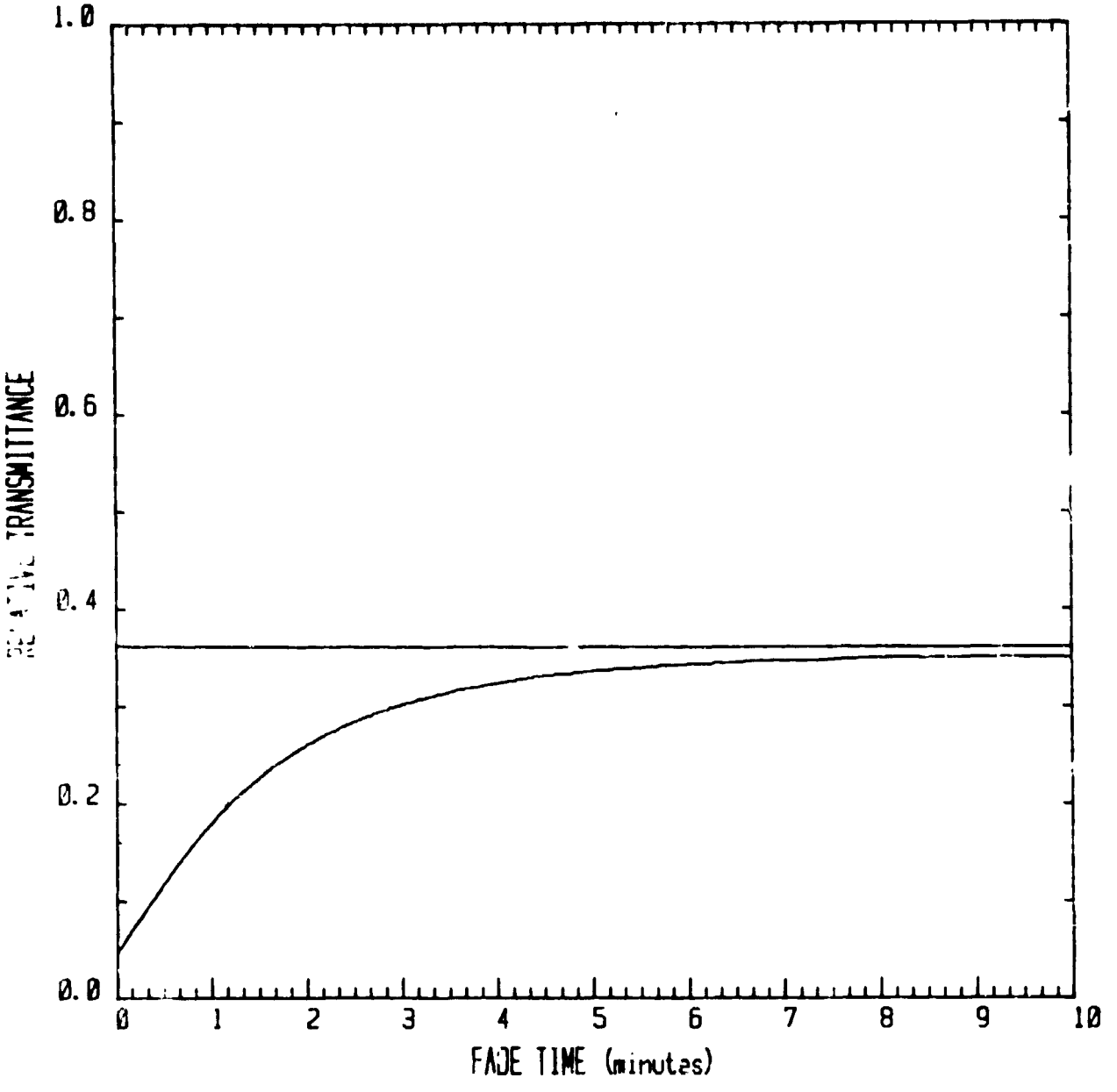

Fade time for a solution of DMSO and a triarylmethane class of photochromic dye (malachite green leucocyanide). Transmittance measured at ~640 nm.

Figure 2.2-6

Table 2.2-4

Characteristics of Photochromic Compatible Fluids

Solvent	Dielectric Constant	Viscosity (cp)	Dissipation Factor (Resistivity)	Coefficient of Expansion ($°C^{-1}$)	Comments
DMSO	47	1.98	(3.3×10^{7} Ωcm)	.00088	
Ethylene Glycol	38	19.9	NA	NA	Too viscous
2-(2-ethoxyethoxy) ethanol	NA	3.85	(4×10^{7} Ωcm)	0.00082	Too viscous
Methylalcohol	33	.597	(2×10^{6} Ωcm)	0.00117	
m-Tolunitrile	~40	~1	0.01	NA	
Acetronitrile	38	0.345	NA	0.00137	
Dimethylformamide	38	0.802	NA	NA	
Cyclohexanone	18	~2.0	NA	0.00091	
Chloroform	4.8	0.571	(4×10^{9} Ωcm	0.00129	

2.2.1.4 Conclusions and Recommendations

Identifying compatible photochromic dye-solvent systems having the high dielectric constant, low viscosity and coefficient of volume expansion desired for the AGCE was shown to be very feasible. The parameter requiring additional quantification before a final selection can be made is the fluid dissipation factor, which is a function of fluid purity. It is highly recommended that the fluid purification and characterization program outlined in this study be completed prior to, or early in the AGCE hardware development. The objective of this program would be to (1) determine what values of fluid dissipation factor are feasible, (2) assist in selection of the optimum solvent-dye system, and (3) establish an operational fluid purification procedure for the AGCE. Candidate fluids should be selected by evaluating the characteristics in Tables 2.2-3 and 2.2-4.

The feasibility of obtaining high dielectric constant solvents compatible with photochromic dyes was demonstrated using available spiropyran and triarylmethane compounds. Of the several triarylmethane-solvent systems evaluated, malachite green lencocyanide in dimethylsulfoxide is probably the most attractive, although it is one of the more difficult solvents to purify and has a relatively high freezing point. The spiropyran-solvent evaluation was more limited in that only two spiropyrans, DMS and TNSB, were available. The DMS compound was designed to have very short fade times (few seconds) and although this compound is not desirable for the AGCE application, it successfully demonstrated the feasibility. The TNSB compound provided fade times of approximately 100 seconds which is within the 1-2 minute range desired for the AGCE. Three solvents having high, medium and low dielectric constants which appear to offer the best compromise between high density and long fade time when used with the spiropyran

photochromic are:

Solvent	Dielectric Constants
m-tolunitrile	40.0
cyclohexanone	18.3
chloroform	4.8

However, as stated above, the achievable fluid purity and dissipation factor will be a critical factor and will require consideration along the dielectric constant in the ultimate fluid selection.

While the solvents identified in this study are commercially available, the photochromic compounds are not and will probably have to be synthesized as needed.

2.2.2 Material for the Outer Sphere

Selection of material for the outer sphere of the AGCE apparatus (PIR No. 1254-AGCE-020) considered the following aspects: (1) material composition, (2) source of material, (3) size obtainable and fabrication technique, and (4) cost and delivery time. Two materials, sapphire and spinel, were initially identified as potentials for the outer sphere. However, spinel was quickly eliminated due to its poor optical quality and its unavailability in the large sizes desired for the AGCE. Emphasis was therefore placed on items (2), (3) and (4) relative to sapphire only.

Crystal Systems, Inc. was identified as the only producer of large sapphire boules of the size required for the AGCE. Presently, material to fabricate hemispherical shells with up to 4 cm inner radius can be provided with the optic axis and centerline co-linear (to minimize the effects of birefringence), while shells with an inner radius of 7.5 cm can be made with the optic axis

perpendicular to the centerline. Larger boules may be available in the future and permit construction of larger shells with co-linear optic axis and centerline. However, as described in Section 2.3.5 and PIR No. 1254-AGCE-027 the image shifts produced by the birefringence are completely predictable functions of latitude and longitude and can be removed through a calibration procedure. Thus, the relative orientation of the optical and centerline axes is not critical as long as it is known.

Estimates for fabrication of the hemispherical shell were obtained from Insaco, Inc. and Frank Cooke, Inc. who both specialize in machining of sapphire. The size and optical requirements which were provided to them are given in Figure 2.2-7 and the results obtained from them are summarized in Table 2.2-5. Machining of the boules into hemispherical shells can be performed by either machinist, although better surface quality is guaranteed by Frank Cooke ($\pm$1 fringe power and 1/2 fringe irregularity vs. $\pm$5 fringe power and 2 fringe irregularity). It is therefore recommended that an assessment of surface quality requirements be performed and used as the basis for selection of the machinist. Total procurement time for producing the hemisphere (production of the boule and machining) may approach or exceed a year.

An alternate option for fabricating the hemispherical shell was suggested by Frank Cooke. Rather than machining the shell out of a single piece of sapphire, a technique similar to that used in constructing a geodesic dome could be employed. This method would allow construction of almost any size dome but at an increased cost. For example, a shell of inner radius approximately 8 cm would cost approximately $100K (telecon estimate from Frank Cooke) assuming it was composed of segments subtending an angle of 10°. This fabrication technique would also require a more complex calibration procedure to eliminate the effects

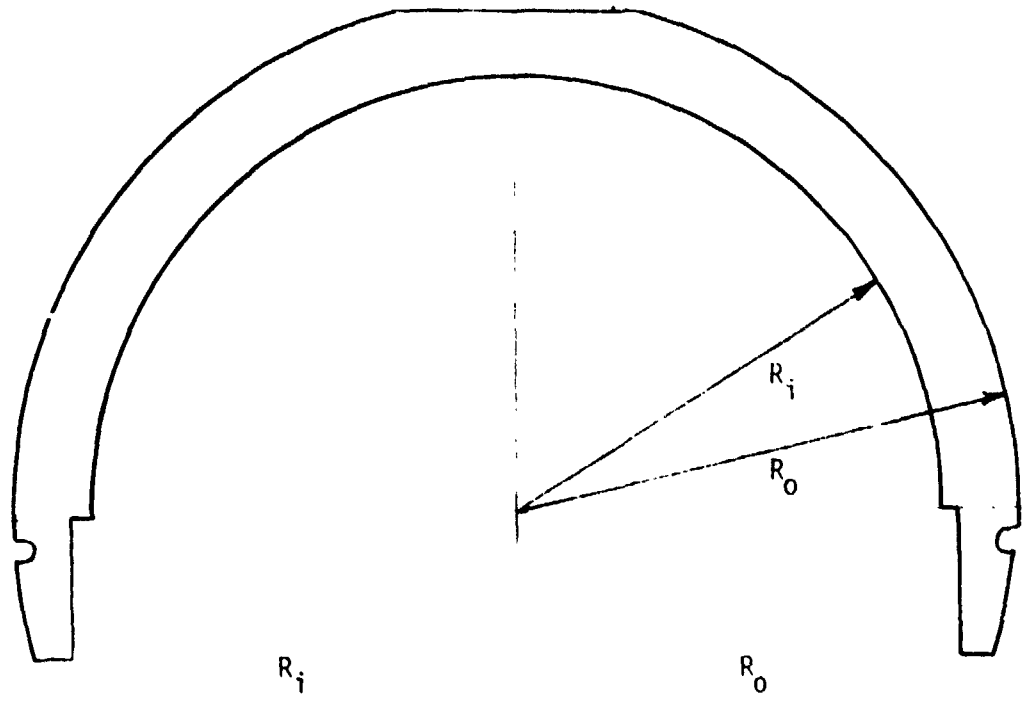

Case 1.	4.00 cm + 0.01 cm	5.00 cm + 0.01 cm
Case 2.	6.00 cm + 0.01 cm	7.00 cm + 0.01 cm
Case 3.	7.50 cm + 0.01 cm	8.50 cm + 0.01 cm

REQUIREMENTS:

1. Edges and bevels to be fine grind.

2. Materials: synthetic sapphire, optical quality. No imperfections or inclusions larger than .010 in diameter permitted. Crystal axis co-linear with indicated centerline within 5°.

3. Scratch and dig 80-50. There shall be no evidence of grayness or stain on optical surfaces.

4. Surfaces of clear aperture shall be test plate fit within 1 fringe power and 1/2 fringe irregularity over a one inch diameter area using a standard mercury source.

5. Clear aperture: I.D. and O.D.

Figure 2.2-7. Hemisphere Size and Optical Requirements Used to Obtain Cost Estimates

Table 2.2-5

Cost Estimates for Material and Machining of the AGCE Outer Hemisphere

	Hemisphere Size		Cost Quotes		
			Sapphire Material	Machining	
	Inner Radius	Outer Radius	Crystal Systems, Inc.	Insaco, Inc.	Frank Cooke, Inc.
1	4.00 cm	5.00 cm	$ 6,000	$12,000	$20,000
2	6.00 cm	7.00 cm	$10,250	$13,750	$25,000
3	7.50 cm	8.50 cm	$17,000	$20,000	$30,000
4	5.35 cm	6.35 cm	$ 9,100	$13,900	-
5	6.00 cm	7.00 cm	$11,000	$15,000	-
6	6.60 cm	7.60 cm	$15,000	$19,000	-

of birefringence, since each segment would require individual consideration. Thus, this fabrication technique should only be considered if sphere sizes achievable by machining a single boule are not adequate.

In summary, it appears feasible to obtain hemispherical sapphire shells of up to 7.5 cm inner radius which will provide the required optical quality for the AGCE. Since the birefringence effects can be calibrated out and since they are significant for deviations as small as approximately 1 mrad between the crystal axis and wave normal (PIR No. 1254-AGCE-027) it does not seem feasible to attempt to eliminate these effects through fabrication techniques.

2.2.3 Dielectric Material for the AGCE Baffle

In the construction of the AGCE assembly, an equatorial baffle may be required in the lower hemispherical section of the convection cell to prevent fluid circulation in that region (PIR 1254-AGCE-016). The dielectric constant of the baffle material should match that of the dielectric fluid to minimize distortion of the electric field.

Since fluids with dielectric constants of 40 or more may be used, the availability of material for the baffle which had this large a dielectric constant was a concern.

A potential source of acceptable material for the baffle in the AGCE assembly is Trans Tech, Inc. of Gaithersburg, MD. They can provide ceramic dielectric material with any value of dielectric constant between 14 and 140 on request. They will also machine the material to customer specified configurations. Data sheets giving complete specifications for several compounds are given in PIR 1254-AGCE-019. Based on the information obtained to date, procurement of a dielectric baffle material to match the dielectric constant of the fluid seems

quite feasible.

2.2.4 Dust Removal

It has been found by Dr. W. Fowlis that dust particles in the dielectric fluid oscillate due to the applied electric field. This oscillation can disturb the activated photochromic dye markers used to assess dielectric fluid flow (within the spherical capacitor test cell) during an experiment. The amplitude excursion of the dust and consequently the disturbing effect is reduced by increasing the frequency of the electric field. The amplitude of displacement decreases inversely as the square of the frequency. This disturbing effect is much reduced for frequencies above 300 Hz. A combination of a high frequency voltage source and filtration of the dielectric fluid should eliminate the problem.

The high voltage power supply described in Section 2.5 has been selected to operate at 300 Hz to help alleviate the dust problem. The present section deals with the filtration of dust after assembly of the AGCE unit.

The key design requirements related to the dust removal capability were generated and based on previous development experience, the Spacelab Payloads Accommodation Handbook SLP/2104 and an estimate of the AGCE flight design (see Section 3.1). These served as guidelines for the feasibility study.

The results of the feasibility effort indicate that a dust removal capability can be readily accommodated. The corresponding weight and peak power required are 1.7 kg and 35 watts respectively. Suitable hardware elements are available for incorporating the capability into the AGCE. Preflight and periodic inflight operation of this AGCE capability is recommended. Purging the internal volume of the spherical capacitor assembly (AGCE cell) can be readily accomplished. The preferred mechanical assembly is shown in Figure 2.2-8.

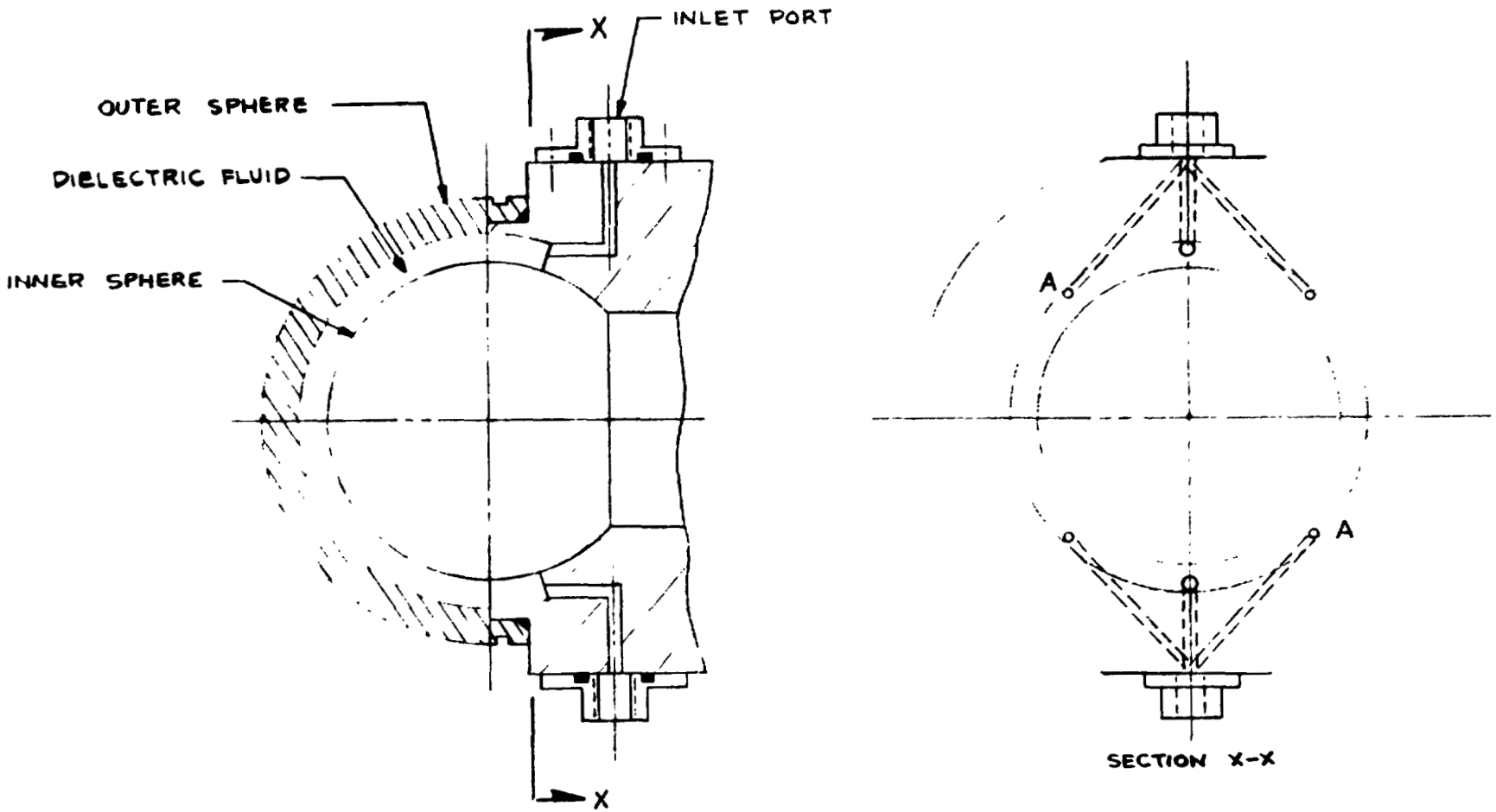

Figure 2.2-8. Inlet/Exist Port Arrangement Without Equatorial Baffle (not to scale)

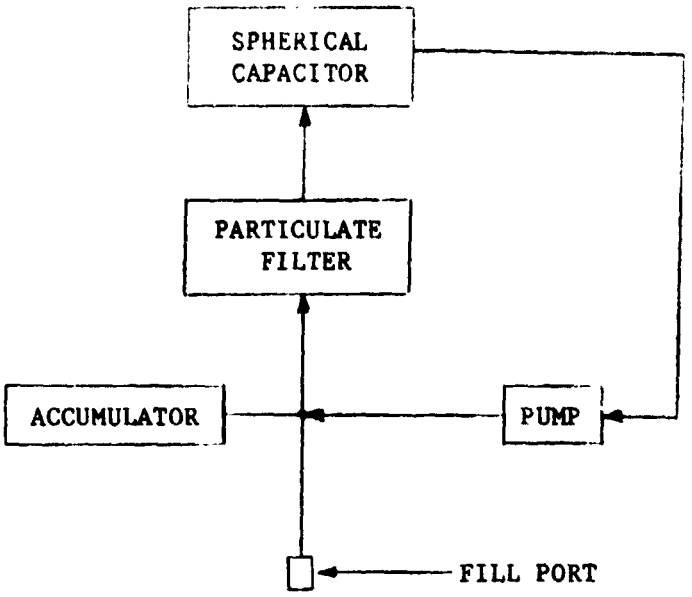

Figure 2.2-9. Filtration and Circulation Loop Block Diagram

Figure 2.2-9 shows the circulation loop block diagram. The dielectric fluid volume is estimated to be 275 cm^3 which assumes the fluid volume does not extend below 10^oS latitude.

The pump selection took into account the coolant flow requirements of the thermal subsystem. A pump candidate is an assembly being used in the Shuttle Galley currently under development by GE for NASA-JSC. This pump is a magnetically coupled gear pump supplied by Micropump, Concord, CA. Use of this pump will result in a circulation flow rate of 1420 cm^3/min (0.375 gpm) and a system operating pressure of 15 psi. At this flow rate and an estimated dielectric fluid volume of 275 cm^3, a 26 volume purge can be accomplished during a 5 minute period. This should be more than ample to maintain the dielectric fluid in a dust free condition.

A disposable depth type filter tube (Type AAQ) available from Balston, Inc., Lexington, MA, appears to be suitable to maintain particulate concentrations in

the dielectric fluid at less than 10 particles/cm^3 for particles exceeding 0.5 micron in diameter with the maximum particle size not to exceed 1.0 micron.

The function of the accumulator is to compensate for the change in dielectric fluid volume due to changes in fluid temperature occurring during the AGCE activity. The maximum temperature range occurs during transportation conditions which for the assumed accumulator design produces a variation in system operating pressure of a minimal $\pm$4.1 psi.

Leakage of dielectric fluid from the dust removal hardware is not expected to be a problem particularly since the suggested pump assembly is a magnetically coupled type, thus eliminating a rotating pump seal.

Materials compatibility with the dielectric fluid should not be a problem but must be re-evaluated against the dielectric fluid finally selected.

Operation of the dust removal capability during AGCE final assembly, acceptance test, pre-launch checkout and on-orbit operations is recommended.

2.3 OPTICS FOR DATA RETRIEVAL

2.3.1 Overview

The objectives of the AGCE are to generate time-sequential maps of both fluid circulation and thermal gradient over substantially a full hemisphere of rotating test cell that models the earth's atmosphere.

This study has shown that the measurement requirements of the AGCE can be met by a relatively simple instrument using a flying-spot scanner. A preliminary design, by no means optimized, has been shown capable of surveying one hemisphere of the rotating test cell at 1^{o} resolution over a 69^{o} span of latitude. This scanner can observe and measure the two non-radial components of thermal gradient in the test fluid with $0.01^{o}C/cm$ resolution at a signal-to-noise ratio (SNR) of at least 6. Photochromic marker dots can be observed simultaneously with a SNR in the hundreds. The same detectors can also feed a closed circuit television (CCTV) display for the payload specialist, with a SNR in the hundreds.

The preliminary optical design developed for this study has been shown through raytracing to exhibit outstanding image quality and to yield a signal that is linear with thermal gradient over at least two decades of dynamic range.

This flying-spot scanner instrument being fundamentally simple in design should be realizable at modest cost. Volume and weight will be small in comparison with the rest of the experimental apparatus.

The study has also shown what direction to take in further improving the design, especially with respect to increasing the latitude scan angle and the signal-to-noise ratio.

2.3.2 Test Cell Configuration and Requirements

In order to proceed with a preliminary design and performance evaluation, it is necessary to assume certain facts and requirements relating to the physical character of the test cell and scanner design that might eventually be imposed. The most important of these are provided in Table 2.3-1. The basic configuration for the test cell is given in Figure 2.3-1.

Table 2.3-1
Test Cell Configuration and Requirements for Design of Data Collection System

Cell Fabrication Tolerances	
Radii	±0.1 mm
Surface Figure	1 ring power 1/2 ring irregularity over 25 mm diameter at 589.3 nm
Scratch and Dig	80/50
Outer Sphere	
Material	Synthetic Sapphire
Optical Axis	within 5° of rotation axis
Test Fluid	
Material	DMSO
Optical Properties	Like Glass 478275
Inner Sphere	
Material	Aluminum
Optical Properties	Specularly reflective like silver
Cell Rotation Rate	0.25 to 3.0 radians/sec
Scan Pattern	6° to 82° along meridian
Scanner Spot Size	1° at sphere center
Scanner Optical Design	Centered on Sodium D-line 589.3 nm
Dynamic Range	0.1°C/cm to 1°C/cm
Gradient Sensitivity	0.01°C/cm
Spot Detection Sensitivity	0.2 of full illumination level
Mechanical Clearance Between Sphere and Scanner	1 mm

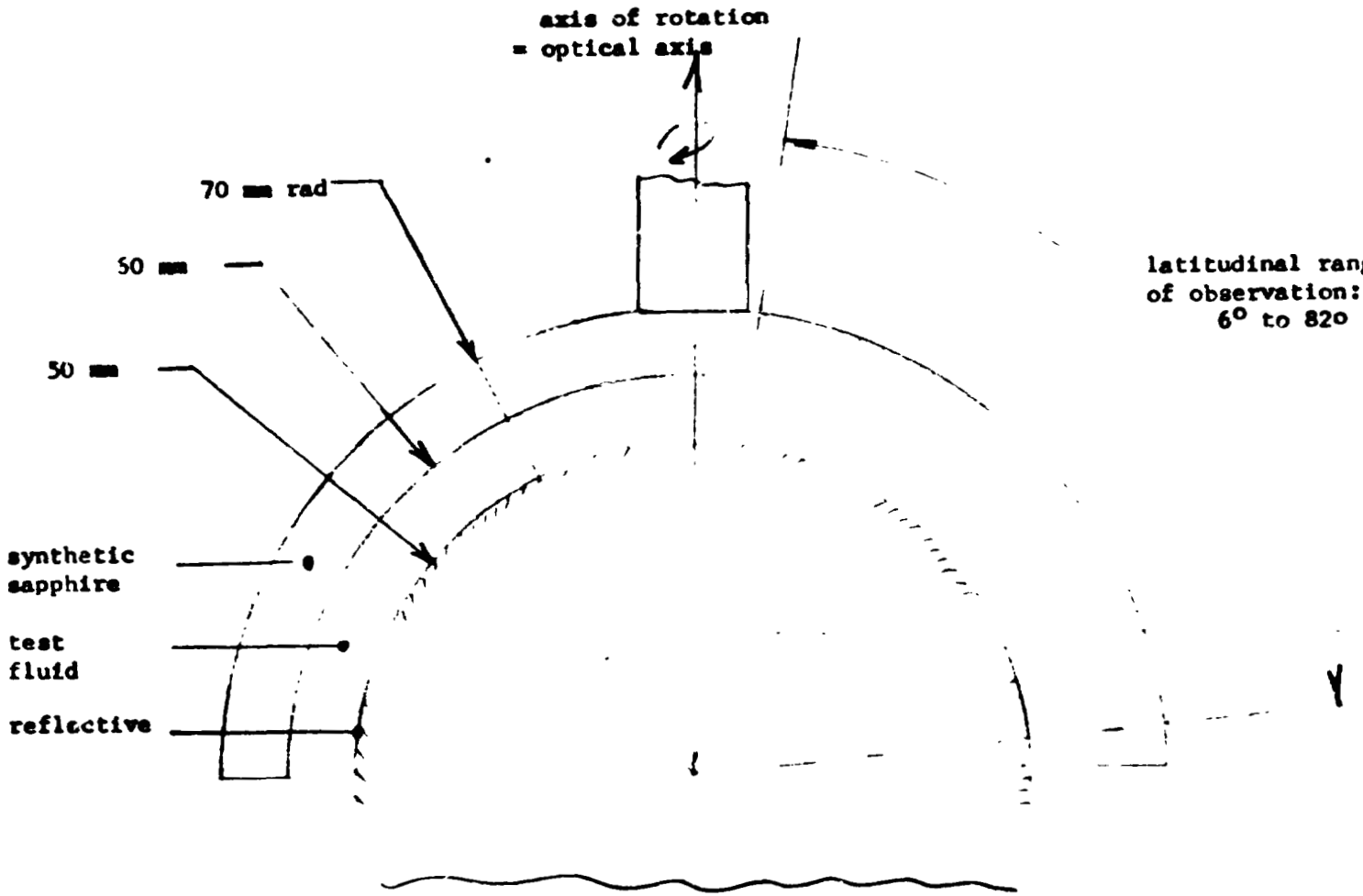

Figure 2.3-1. Assumed Basic Configuration of AGCE Test Cell

2.3.3 Design Approach

A direct and accurate method of thermal mapping employing a flying spot scanner can take the form illustrated in Figure 2.3-2. In this system the virtual image of the reflective inner surface is projected to infinity by a second, concentric mirror. This monocentric pair generated by an Offner relay can image a target near the common center at unit magnification in a manner substantially free of all third order aberrations. When this target is illuminated by a rotating collimator sharing the same vertical axis, the light passing through the target will be brought to a sharply focussed spot on the inner reflective sphere, then returned to the target image. As the illuminator rotates, the scanning spot will sweep out a thin arc of a great circle on the surface of the inner sphere. If thermal gradients (manifested as refractive index gradients) are present in the fluid, the light passing through the focussed spot will be significantly deviated in direction, but the location of the spot will be only slightly affected. The result is that the direction of the rays returning to the target image will be altered only very slightly, but the target image itself will translate significantly. This translation is two-dimensional and directly related to the magnitude of the thermal gradient vector. Two orthogonal components of the index gradient vector can be measured directly, in terms of image displacement, by a four quadrant detector array placed at the target image position (see Figure 2.3-3). Since simultaneous encoder readings identify the surface location of the flying spot, all information needed to develop a surface thermal map is available directly in electrical form, suitable for electronic recording or transmission.

This instrument has the further advantage that it can also perform the surface flow mapping at the same time it does the thermal mapping. Surface flow is

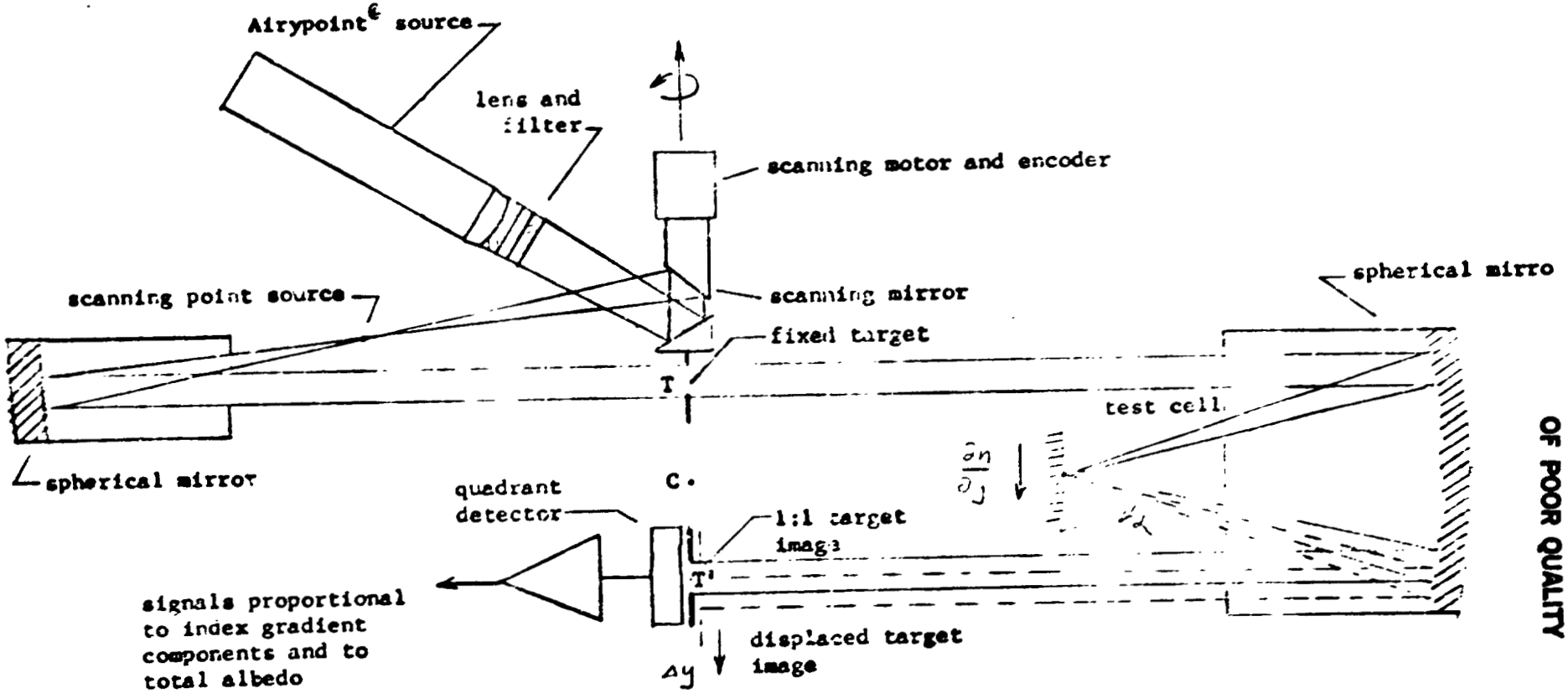

Figure 2.3-2. Thermal Gradient Measurement Concept (unfolded)

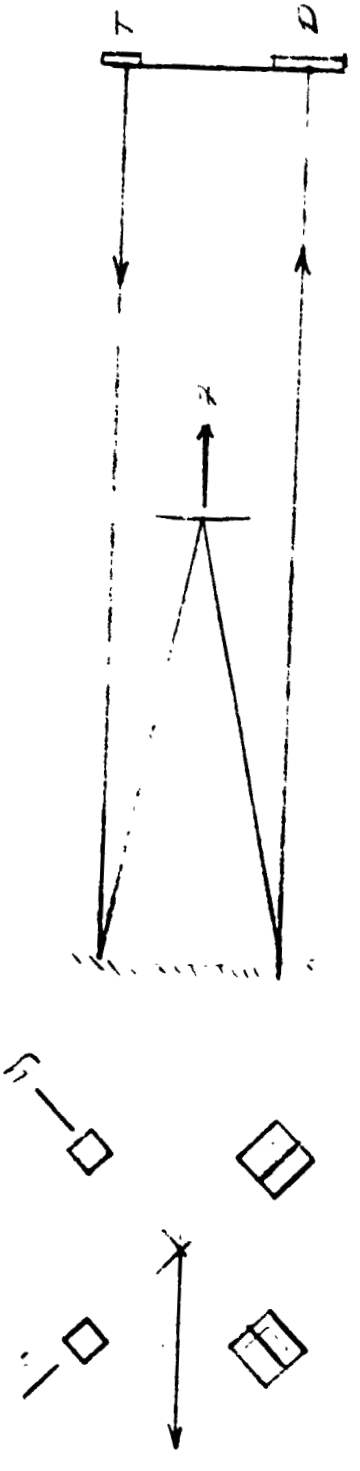

Figure 2.3-3. Selected Target-Detector Configuration for Preliminary Design

described entirely in terms of the drift in a matrix of photochromic markers in the fluid. Any means of locating a marker dot in both surface coordinates and time can therefore accomplish flow mapping. The flying spot scanner just described can do exactly that. In this case one would make use of the total return at the four quadrant detector, whose magnitude is a measure of surface albedo. A sudden drop in that total signal, detected by a differentiation circuit, identifies the presence of an opaque marker dot at the locus of the scanner spot. If then both deflection signals and total signal derivative are recorded simultaneously with scanner and model encoder signals, both surface flow and surface thermal maps will have been recorded in a form lending itself to subsequent automatic processing and plotting.

The flying spot scanner can also furnish the payload specialist with a substantially real-time synoptic view of the surface. The scanner sweeps an entire hemisphere in the form of thin meridional zones. Each scan can be displayed as a single vertical line on a video display that is scrolled sideways at a rate corresponding to the model rotation. The payload specialist would then see on the screen a slowly scrolling display of the entire hemispherical surface in cylindrical equal-spaced projection. This has the merit that it uses essentially raw signal, conditioned only enough to match the display electronics. If for human engineering or other reasons another type of projection or display is preferred, the raw signal can of course be processed locally to provide it.

2.3.4 Baseline Design

The flying-spot scanner of Figure 2.3-2 is based on the monocentric (Offner) relay. The optical path has been folded away (Figure 2.3-4) from the test cell itself, to avoid physical interference. The folding mirror (or mirrors) has t

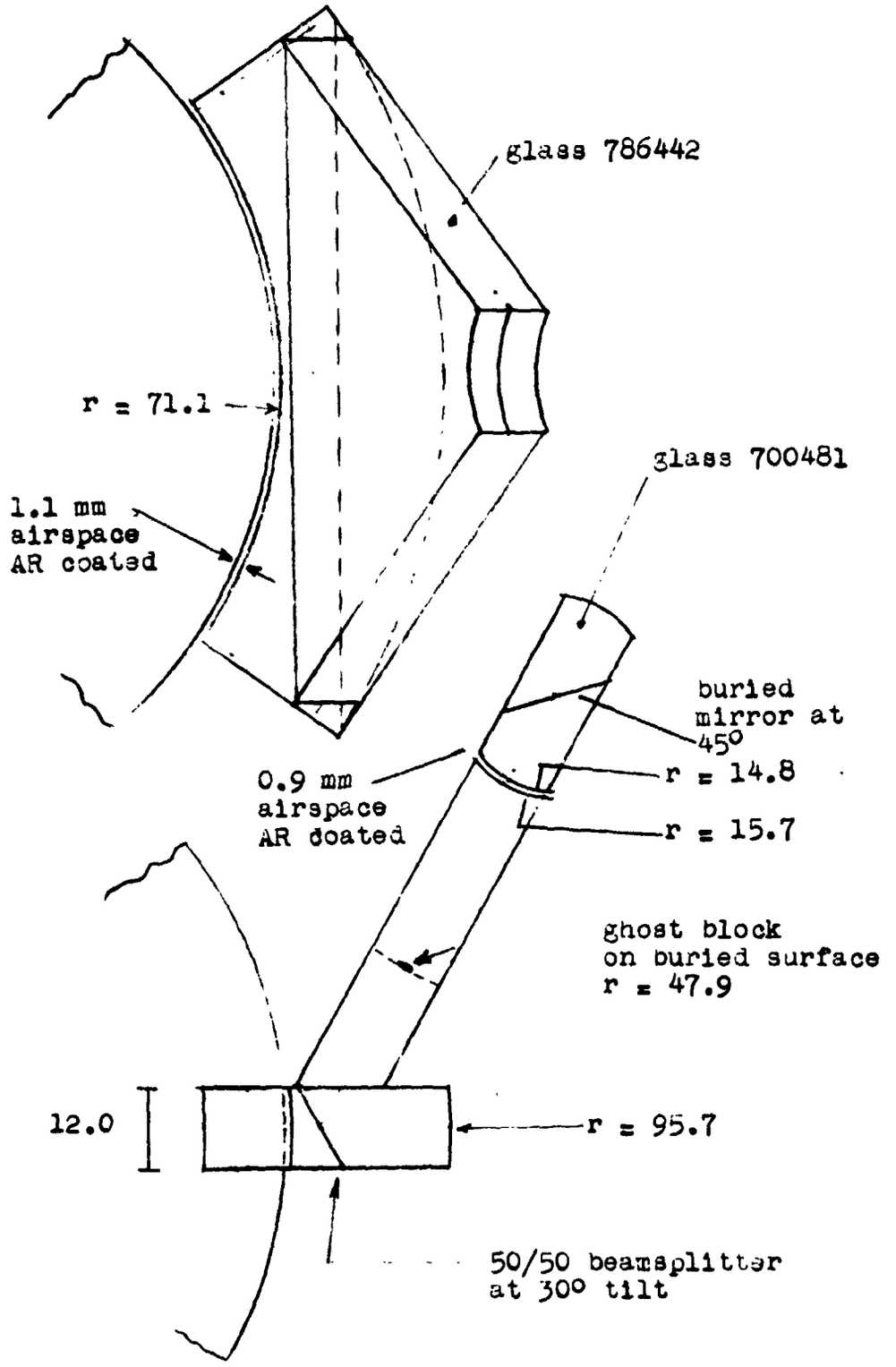

Figure 2.3-4. Folded Scanner Relay

chosen to be semi-reflective because it maximizes the scan angle and allows the scanning beam to pass through the test fluid almost radially. This is important for minimizing the volume of fluid intercepted by the scanning beam and therefore maximizing the spatial resolution of the instrument. On the other hand, a semi-reflective folding mirror will entail a substantial loss of light and will introduce ghosts that must be blocked or absorbed.

As seen in Figure 2.3-4, the monocentric relay is implemented using a solid glass design assembly because it results in a smaller and more stable instrument, is easier to realize the semi-reflective folding mirror as a buried-surface beamsplitter, and fresnel losses can be better controlled. On the debit side of the ledger, it must be admitted that a solid system is generally harder to make, will reduce the deflection produced by any given thermal gradient and will reduce the available scan angle. Its advantages outweigh its disadvantages.

To realize a solid system while allowing for motion of the test cell and the scanner head, a zero-power air lens has been introduced at the two interfaces where relative motion will occur: (1) between the scanner assembly and the test cell, and (2) between the scanner head and the scanner body. We visualize each interface as two concentric spherical surfaces separated by a small air gap of about 1 mm. The glasses are chosen so that the optical power of the thin air is zero.

Detectors considered for the allowed detector configuration include the following: UPT PIN Spot/2D and Hughes HPIN 100D, which are both available as chips. The basic design constraint is the chip size to accommodate the image height at the center of 3.30 mm and fit physically close to each other in a four quadrant arrangement.

The solid Offner relay has been designed to be achromatic over the normal visible spectrum. The nominal relay design has been based on the mid-image height (3.30 mm) and the sodium D-line (5893 angstroms). This nominal design results in a selection of glasses on the basis of sodium D-line index n_D. Normally several glasses will be available with very nearly the same n_D but with different dispersive properties, expressed in terms of the Abbe V-number which can satisfy the requirements for achromatization.

Considerations of both the illumination spot size and the achievable scan angle led to some mutual exclusive physical constraints for the selected target/detector array. The ray envelope which must be accommodated at the primary mirror is 10 millimeters in diameter when a 1x1 mm target with its attendant motion from index gradients is to be used. This envelope as it traverses the optical assembly will allow only a 69° scan while still permitting all light to reach the primary mirror via the folding beamsplitter and while having the entire envelope clear the mirror.

Improvements in the baseline design can increase the achievable scan angle. Such improvements include a more compact target/detector array, a larger radius for the primary mirror, and lowering the index of refraction for the glass forming the main body of the relay.

The rapid rotation rate (10,300 RPM) on the scanner head which is necessary to handle the cell rotating at its maximum rate of 3 rad/sec makes it impractical to attempt putting electrical power in or out of the head while in motion. The detector therefore can not be physically mounted on the scanner head. The solution used, as seen in Figure 2.3-5, is to use Offner relays to put images of source and detector onto the scanner head. The scanner head incorporates a fully reflective buried folding mirror that will rotate these images into the self-

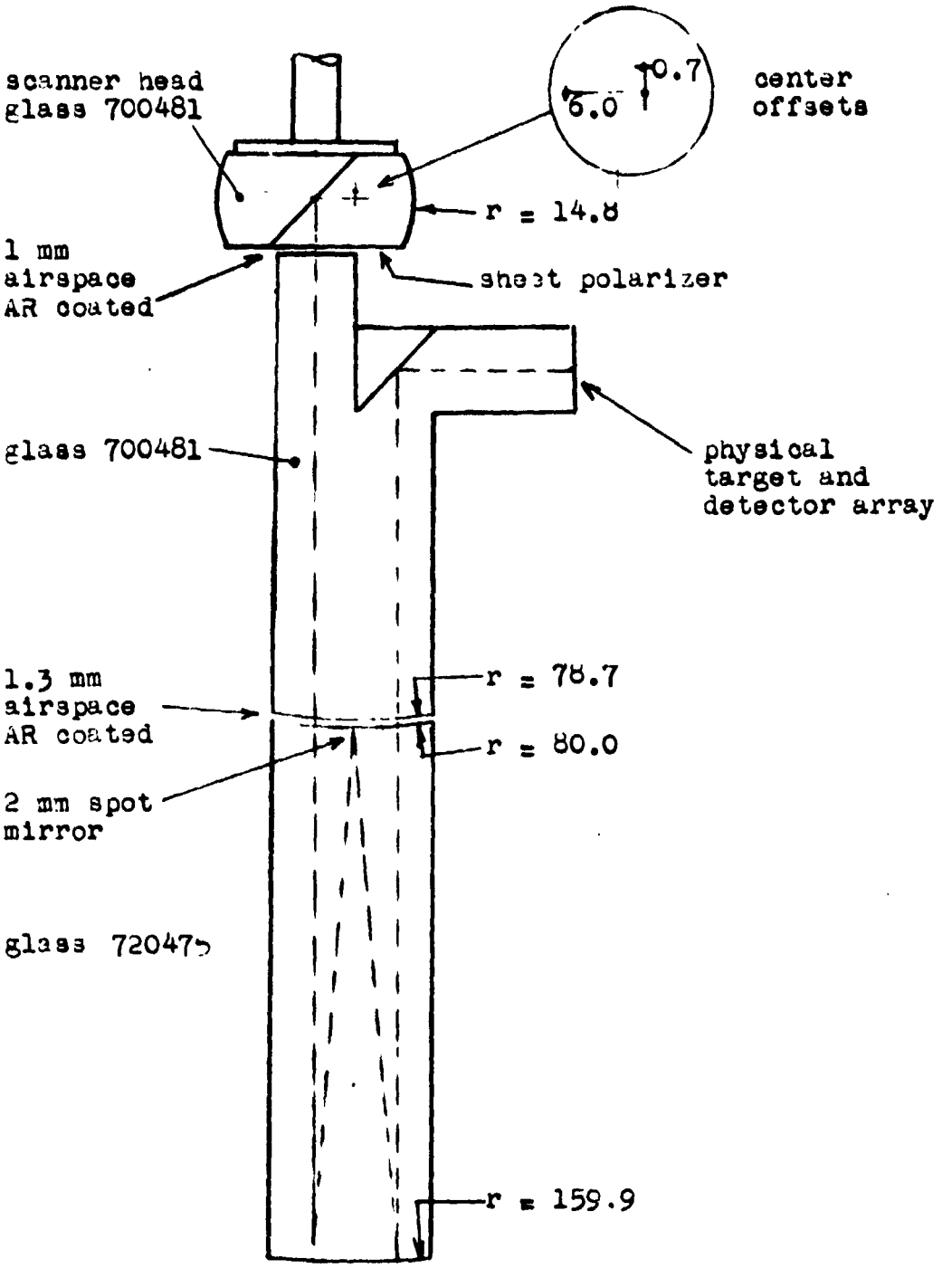

Figure 2.3-5. Input Relay to Scanner

conjugate plane. There they will function exactly as would physical sources and detectors. The only part that moves, now, is the small glass scanner head, which should be made symmetrical for dynamic balance.

If the source/detector assembly is fixed, as we would recommend it to be, the apparent orientation of this array changes as the scanner head rotates. The detectors continue to record two orthogonal components of gradient, but the reference axes rotate over the course of the scan. This rotation of axes is systematic, however, and is known a priori very accurately. Since an encoder signal will record scan latitude, the same encoder is also recording the rotation of the array axes. Hence there should be no trouble in transforming indicated components to any axes desired, as part of the normal reduction process.

The advantages of the semi-reflective folding mirror carry with them the presence of ghosts. These are not difficult to eliminate, however. Ghosts created by the folding mirror can be diverted, absorbed or blocked. The most important ghost is a replica of the focussed spot that appears at the ghost image of the inner reflective sphere. This could be eliminated very simply by placing the scanner head interface at that ghost image and physically blocking the light with a black spot on the glass. In the present case this would make the scanner head larger than is desirable for dynamic reasons, so instead we provided a buried surface at that point which occurs in the scanner relay and block the ghost with a black absorbent stripe on that surface (see Figure 2.3-4). The zero-power interface can then be placed so as to minimize the size of the scanner head.

Applying the procedures and considerations detailed above, we arrived at the complete preliminary scanner configuration shown in Figure 2.3-6. This

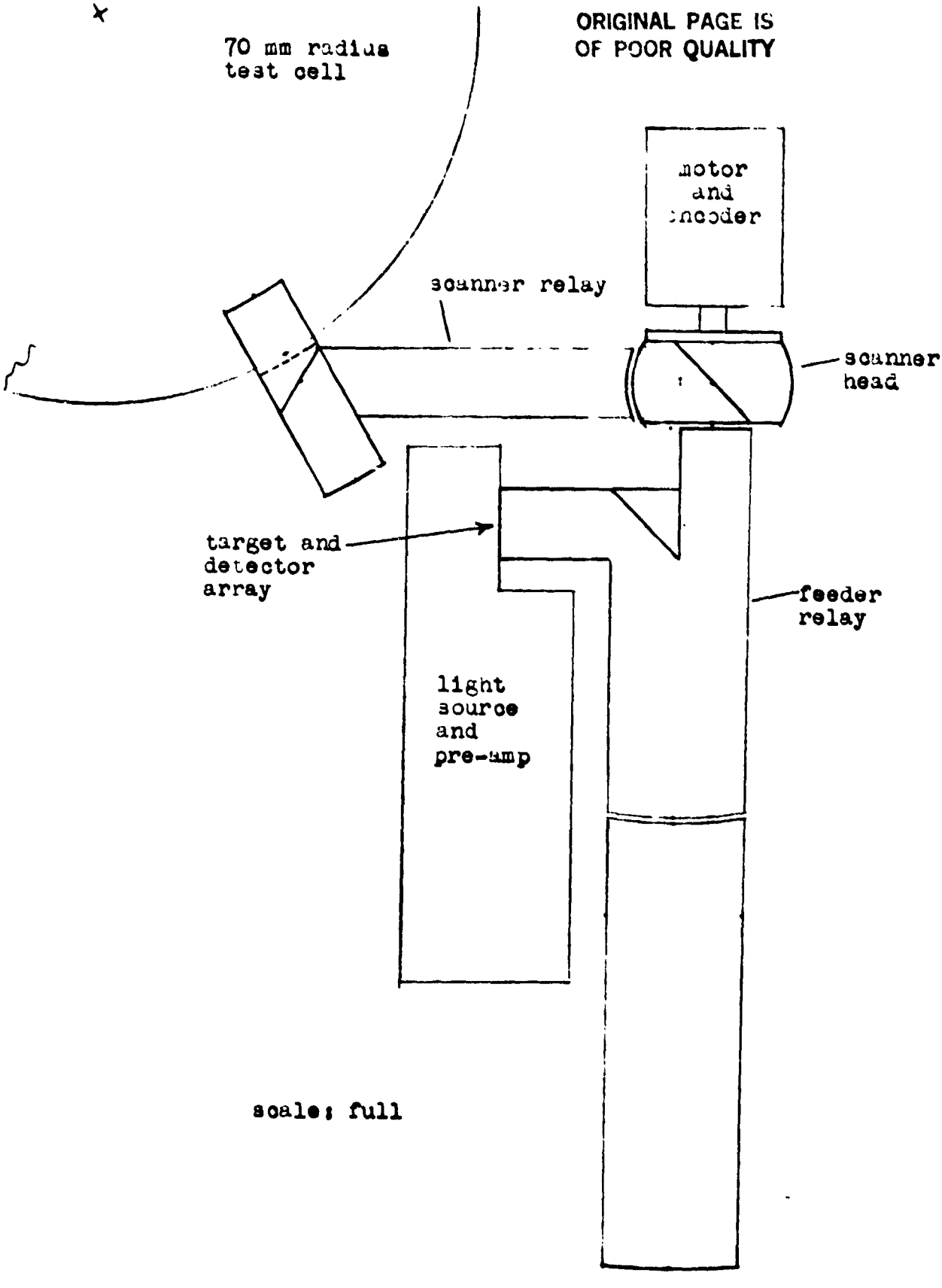

Figure 2.3-6. General System Layout

instrument promises to be realizable at reasonable cost, to be stable and reliable in use, and to yield the results desired.

2.3.5 Performance Characteristics

The baseline design as defined in the previous section was analyzed to ascertain whether the image quality was satisfactory and whetner the sensitivities to thermal gradient and marker dot opacity are consistent with design goals. The image quality was assessed using ray tracing computational methods. Instrumental sensitivity was determined by photometric analysis.

The results of this analysis are given in Table 2.3-2. A comparison with the requirements given in Table 2.3-1 indicates a very favorable relationship to the designed performance goals.

Improvements in both the achievable scan angle and SNR for thermal gradient while presently adequate can be enhanced for better performance margin. The procedures for their improvement have been identified and documented in Volume II of this report.

One source of optical difficulty for any AGCE apparatus is that for thermal reasons the outer shell of the test cell must be made of sapphire and sapphire is birefringent. Unpolarized light incident on the sapphire shell will therefore be separated on entering the crystal into two rays of orthogonal polarization: the ordinary ray and the extraordinary ray. Since this separation of rays in the crystal can lead to two separate images at the detector, one of which may be displaced from the other, it is evident that birefringence can to this extent mimic thermal gradients, and must therefore be eliminated or taken into account.

The flying spot scanner sweeps the test cell always in thin meridional arcs.

Table 2.3-2

Predicted Performance Characteristics for AGCE Optical Scanner

• Image Quality (Ray Trace Analysis)	
• f/50 Bundle of Rays	
• Diffraction Blur	43 microns
• Geometrical Image RMS Blur	0.04 microns
• f/5 Bundle of Rays	
• Diffraction Blur	4.3 microns
• Geometrical Image RMS Blur	4.2 microns
• Linearity in Image Shift (over 2 decades range for thermal gradient)	1 part in 1000
• Maximum Detectable Shift	414 microns or 12.8°C/cm
• Minimum Detectable Shift	∿0.05 microns or 0.002°C/cm
• Photometric Sensitivities	
• System Transmission (Source to Detector)	1.07%
• Signal Bandwidth	30,940 Hz
• Target Illumination (10 watt Source)	42 microwatts
• Signal-to-Noise Ratio: Full Signal on One Detector	9827
• Signal-to-Noise Ratio: Detection of 0.01°C/cm Shift	6.3
• Signal-to-Noise Ratio: Marker Spot Detection	49

This fact can be turned to advantage in eliminating birefringent effects when the optical axis of the crystal is parallel to the axis of rotation. Since all scanning rays are substantially in the meridional plane, they must also then lie in the principal plane of the crystal. If we then polarize the scanning beam perpendicular to the scanning plane, which is technically easy to do, all rays will appear to the crystal as ordinary rays and birefringent effects will have beem eliminated. This situation was assumed for the baseline design.

The exact alignment of the optical axis with the axis of rotation can not be guaranteed however to closer that 5 degrees because of limitations in the sapphire production process. The birefringent effects occuring because of this misalignment were analyzed. In addition, the use of a sapphire test cell with a radius beyond 4 centimeters requires the production of the crystal with its optical axis in the equatorial plane of rotation where birefringent effects will be increased. The magnitude of these effects were analyzed also.

The conventional approach to understanding the propagation and refraction of light waves is to apply Huygen's principle in its broadest sense. This was done to perform both a preliminary analysis and a detailed ray tracing to identify the magnitude of the birefringent effect. The result of this analysis indicates that in general an image deflection will occur in the direction of the optical axis of the sapphire and have a magnitude of:

$$\Delta = 0.32 \ (\sin \alpha \cos \alpha) \ \text{nm}$$

where α is the angle in radians between the extraordinary wave normal and the optical axis.

In the flying spot scanner, analysis indicates the lower limit for accurate measurement is a deflection of 0.32 microns. An extraordinary image will show this much deflection when α is only 0.001 radians. It appears impossible

therefore to avoid significant image displacements from birefringent effects no matter how the optical axis is oriented, if unpolarized light is used.

However with the optical axis of the sapphire fixed relative to the axis of rotation, the birefringent effect will be completely predictable as a function of latitude and longitude. The effect can therefore be removed through data processing or possibly the use of polarized light tied to the rotation of the sphere. Detailed design studies in the future must take this into account.

2.4 THERMAL ANALYSIS AND DESIGN

2.4.1 Thermal Analysis

A detailed study of localized thermal loading on the inner sphere was performed to establish the feasibility of achieving the desired thermal gradients and to identify the requirements for design of the thermal control system. The study was accomplished by explicit modeling of the fluid motion using a 53 node thermal model configured as shown in Figure 2.4-1 where node divisions occur every 10 degrees of latitude.

The fluid was divided into three layers to represent the flowing fluid. Meridional flow only occurs in the outer layers while radial flow only occurs in the middle layer. Also the fluid is restricted to flow only in the northern hemisphere of the model. Positive meridional flow is in the direction of the pole and positive radial flow is in the direction of the inner sphere. By specifying the total mass flow rate of the circulating fluid in the convection cell and the percentage of radial flow at each middle layer node, various velocity profiles can be established. The mass flow rate at each node is determined by applying the principle of conservation of mass flow. Although silicone oil was used as the fluid, the leading candidate fluids have properties sufficiently close to make the study results applicable to their use.

Because of the relatively low velocities in the circulating fluid, it was assumed that heat is transferred from the fluid to the spheres' surfaces by both convection and conduction. All nodes are radially and laterally (meridionally) conductively coupled as if the fluid was stagnant. The outer layers' convection coefficients were determined by analyzing the meridional flow as flow over a cylinder. The total couplings from the fluid to the inner and outer spheres'

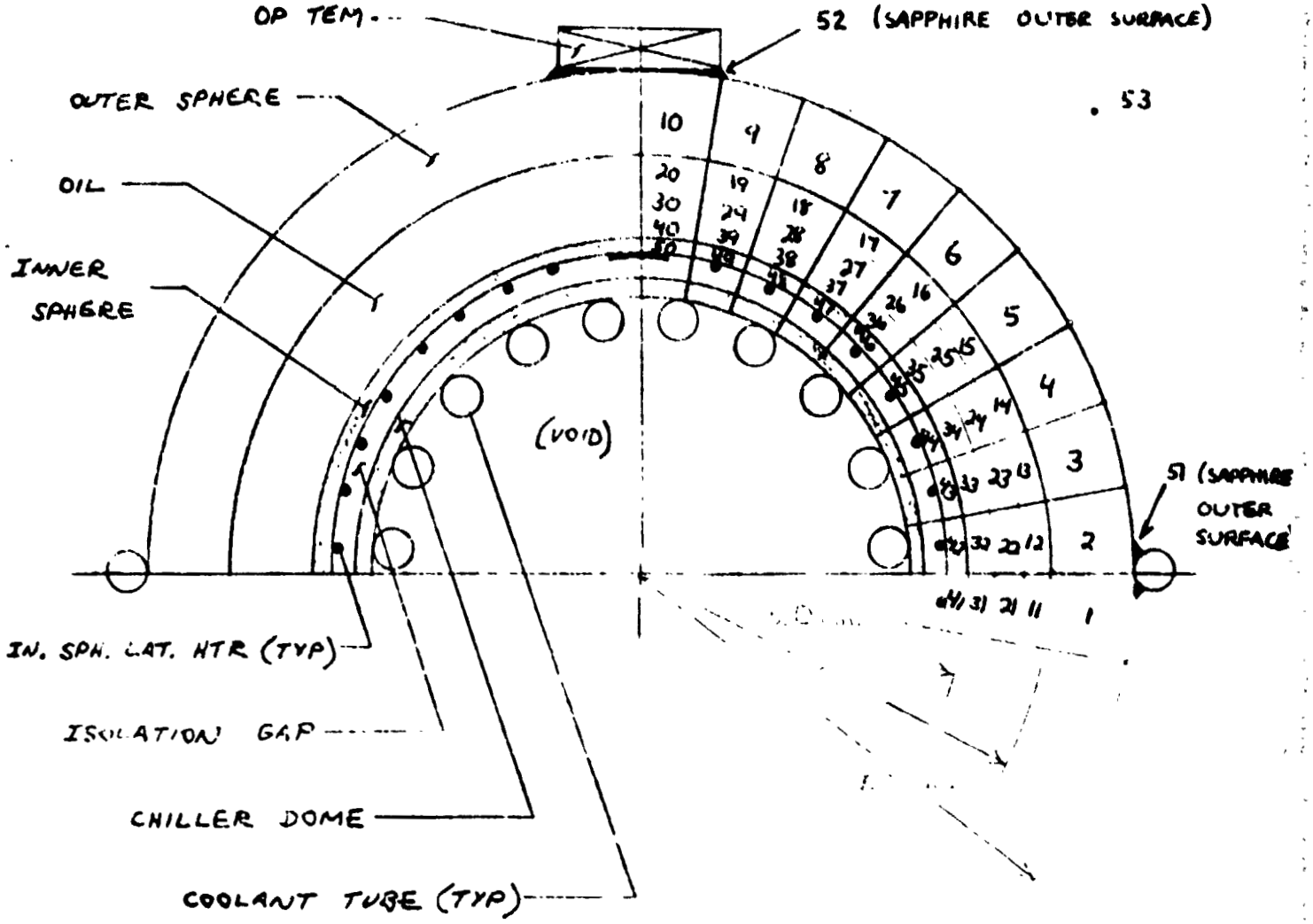

Active Nodes	Description	p (g/cm^3)	Cp (cal/g-°C)	K (cal/cm-sec-°C)	μ (cps)
1 → 10	Sapphire Outer Sphere	3.98	0.10	0.065	N/A
11 → 40	Silicone Oil Dielectric Fluid	1.101	0.47	0.00025	1.98

Boundary Nodes	Description
41 → 50	Inner Sphere
51	Outer Sphere Equator
52	Outer Sphere Pole
53	Ambient Nitrogen Gas

Figure 2.4-1. AGCE Flow Cell Thermal Model

surfaces are the effective couplings of conduction and convection couplings in parallel.

The results of the computer runs for four temperature distributions with various velocity profiles define the heating and/or cooling requirements at the outer sphere pole, outer sphere equator, and all latitudes of the inner sphere and are summarized in Table 2.4-1. Examination of the results shows that the thermal requirements are more dependent on the velocity profile or temperature distribution than the velocity magnitude. The largest total inner sphere cooling load is approximately 7.5 watts (when the entire inner sphere is held at 15°C, Case IIIA). This is also when the greatest heating load is required, approximately 14.0 watts, because the equator must be held at 35°C while the inner sphere is 15°C.

Case IVA illustrates the maximum pole heating load of 5.28 watts required when the pole temperature is 35°C and the flow reversed; simultaneously 1.86 watts of cooling is required at the equator. The AGCE thermal system described below is intended to accommodate these worse case thermal load conditions.

2.4.2 Thermal System Design

A feasible AGCE thermal system is shown in Figure 2.4-2. The inner sphere temperature is controlled by a combination of trim heaters and a hemispherical heat sink (chiller dome) positioned inside the inner sphere, with a gap between the inner sphere and the heat sink. The gap provides partial thermal isolation between the heat sink and the inner sphere. By operating the heat sink at a temperature somewhat lower than the minimum desired for the inner sphere, the heat sink applies a bias cooling to the inner sphere. This bias cooling is offset as desired at each latitude by feed-back controlled trim heaters on the

Table 2.4-1

Heating and Cooling Loads Summary

Case*	Total Inner Sphere Cooling (watts)	TEM Cooling Outer Pole (watts)	Outer Equator Heating (watts)
IA	4.61	3.72	10.52
IA'	4.65	3.72	10.56
IB	3.40	4.05	9.58
IC	4.57	3.52	10.94
ID	2.54	3.81	8.49
IIA	5.88	-1.11	7.04
IIIA	7.49	3.30	13.90
IIIC	7.41	3.20	13.23
IVD	1.90	-4.90	-1.86
IVA	5.31	-5.28	-1.86

*Numbers refer to temperature distributions:

	IP	IE	OP	OE
I	15°C	25°C	25°C	35°C
II	15	25	35	35
III	15	15	25	35
IV	25	15	35	25

Letters refer to velocity profiles (D refers to the stagnant flow case).

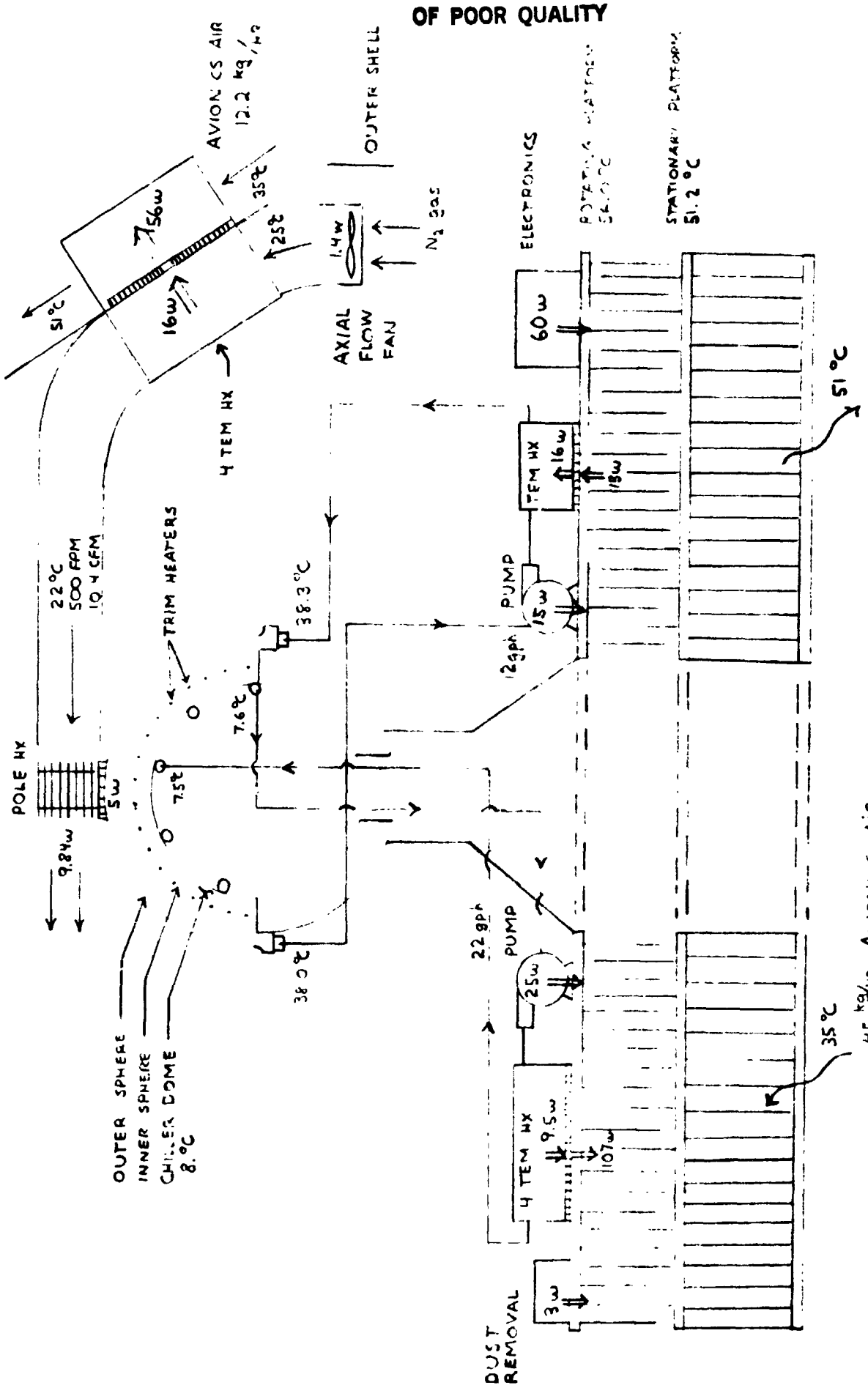

Figure 2.4-2. AGCE Thermal System

inner sphere (every 10^{o} between 5^{o} and 85^{o} latitude). Thus the heat sink serves to cool the inner sphere below the temperature desired at any latitude and the trim heaters provide local heating at each latitude (partially offsetting the heat sink bias) to achieve the desired local inner sphere temperatures.

Both the inner sphere heat sink and the outer sphere equator temperatures are maintained by the use of thermoelectric modules (TEMs) in combination with a pumped coolant. Each cooling loop is operated independently and can supply or remove heat from the equator and/or inner sphere heat sink as required. The outer sphere pole temperature is controlled directly by a convection cooled TEM mounted at the pole location; both heating and cooling can be provided. Overall heat rejection is to the Spacelab avionics airflow via a rotating heat exchanger (similar to that used in the GFFC system) for the turntable mounted elements and by a TEM/blower arrangement for rejecting heat from the pole TEM (as well as heat dissipated to the internal AGCE atmosphere).

Temperature sensors are required on the inner and outer spheres to control the heating or cooling at the outer pole, outer equator and inner sphere. In all three locations the thermal loading can be regulated by temperature sensor feedback to adjust the voltage or current to the TEMs as required. By reversing the polarity of the voltage and current input to the TEMs, they can function in either the heating or cooling modes. This will be necessary when the convection cell circulation is reversed (Case IV temperature profile).

In summary, the thermal design study results show that a thermal system can be designed to maintain the desired flow cell temperature conditions. Although design feasibility has been established, further refinement is necessary for an optimum flight design. It is also recommended that the flow cell operating temperatures be increased 5 to 10^{o}C to provide a more efficient heat rejection

relationship with the Spacelab avionics air flow.

2.5 HIGH VOLTAGE POWER SUPPLY

2.5.1 Requirements

The AGCE power supply is required to deliver a 15 kV RMS sine wave voltage, with an amplitude accuracy of ±3% and a waveform distortion of less than 4%. Multiple settings (100-200) of the high voltage level are required and should be controlled by the microprocessor. The input power will be taken from the available Shuttle system.

2.5.2 Design Philosophy

The large step-up ratio (28 volts DC from the Shuttle to 15 kV for the AGCE) is best handled by employing a series resonant circuit which takes advantage of the resonant rise in voltage. The capacitance of the sphere, with the fluid, has been calculated to be 1.802×10^{-9}F. Therefore the series inductance necessary to resonate at the desired operating frequency of 300 Hz is 156 henries. A preliminary design of this inductor has been completed. The design incorporates a tape core with a high magnetic field saturation level permitting the inductor to be used on the linear portion of its hysteresis loop which is necessary to achieve waveform linearity. The spacing and configuration of the inductor wire has been selected to fit the available volume and to minimize the likelihood of internal voltage breakdown.

2.5.3 Circuit Description

The conceptual circut is shown in Figure 2.5-1. It consists of the following: a series resonant circuit, a driver stage, a voltage controlled gain amplifier, a voltage controlled oscillator (VCO), and feedback signals to maintain the proper frequency and amplitude of the voltage.

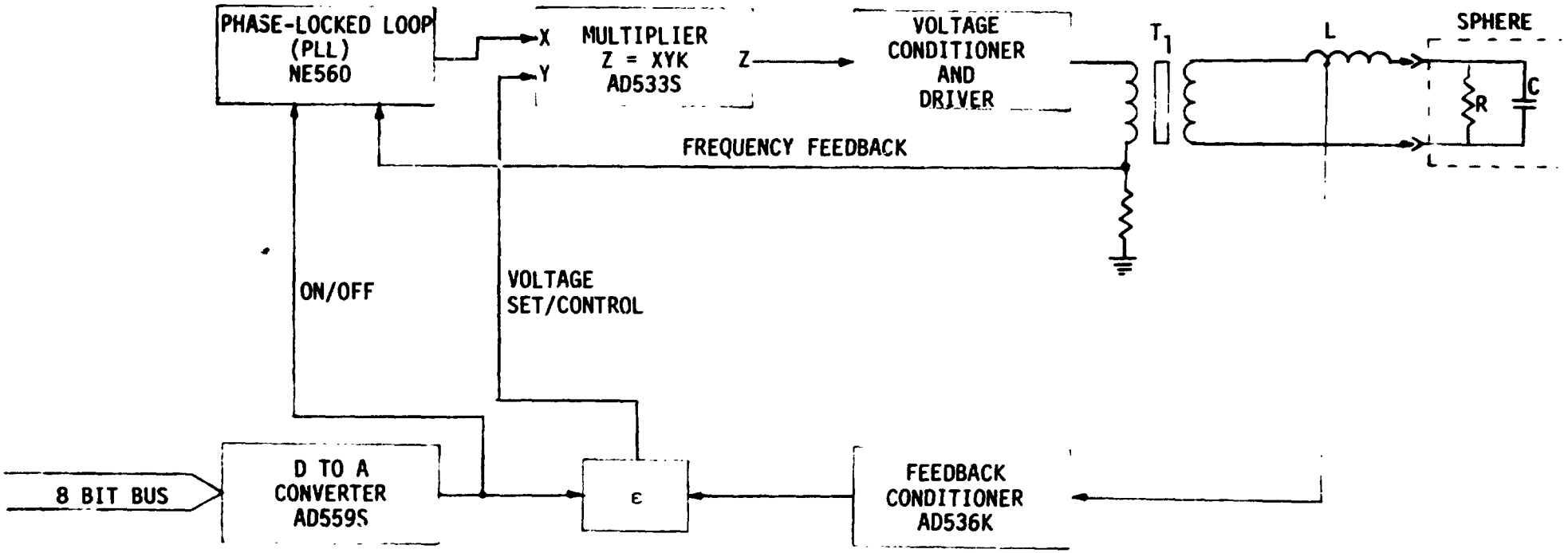

Figure 2.5-1. Power Supply Block Diagram

The VCO, which is part of a Phase-Lock Loop (PLL), is used to generate the 300 Hz. Its output is fed into a multiplier which is used as a voltage controlled gain amplifier, the function of which is to control the output voltage level. The output of the multiplier is then fed into a signal conditioner and onto the driver stage. The driver stage contains a small step-up transformer whose secondary is used to drive the resonant circuit. A current signal is generated in the primary of the transformer and fed back to the input of the PLL. This assures that the circuit will be operated at resonance at all times. A tap on the inductor is used to monitor the high voltage output. This signal after proper conditioning is fed back to the multiplier to maintain the proper output level. It should be possible to obtain the 100:1 dynamic level adjustment by using only the multiplier as the control device. Some testing will be necessary to confirm this.

Information to set the desired voltage level can be obtained from the on-board microprocessor. This information is fed to a digital/analog (D/A) converter whose output is summed with the error feedback signal and presented to the multiplier, which in turn regulates the high voltage output. Up to 256 voltage levels are possible with a single 8 bit D/A converter.

2.5.4 Physical Description

The physical dimensions for the inductor are 8-3/16" L x 4-3/8" W x 5-1/4" H, occupying 188 cubic inches. The inductor is estimated to weigh 3.5 kilograms. The associated electronic package should not exceed 4-3/8" L x 4-3/8" W x 2-1/2" H, occupying 48 cubic inches and weighing about 1.0 kilograms.

With the exception of the inductor which must be custom made, all the components for the high voltage power supply are stock items.

2.6 EXPERIMENT CONTROL AND DATA HANDLING

The type and quantity of data to be generated by the AGCE played a key role in the selection of the philosophy for experiment control and data handling. The AGCE data, unlike that for the GFFC, are in electronic form and being generated at a relatively high rate. In a trade-off study between on-board electronic video recording and telemetry, telemetry was judged to be the better approach because it produced a simpler, less costly flight package and allowed for a more direct role on the part of the principal investigator (PI) during the course of the flight.

On-board recording not only requires a video recorder and interfacing circuitry but also suitable displays and controls for the payload specialist (PS) to assess and control performance. In flight form, this equipment adds substantially to the cost of the flight system and minimizes PI involvement. In contrast, telemetry of experiment data to the Payload Operation Control Center (POCC) permits a shift in roles of the PI and PS such that the PI directly assesses and indirectly, via the PS, controls system operation. Thus the telemetry mode does not require on-board displays; rather these displays reside in the AGCE Ground Support Equipment (GSE) which will be used in qualification and acceptance testing as well as for PI use at the POCC. Table 2.6-1 summarizes the data handling and control philosophy recommended for the AGCE.

Figure 2.6-1 shows a AGCE electrical system functional block diagram incorporating the above data handling and control philosophy. The electrical system provides for microprocessor control of the several thermal control loops, two motor speed control loops, control of the high voltage power supply, data acquisition, data formatting and delivery to Spacelab for telemetering to the POCC.

Table 2.6-1

AGCE Data Management, PS/PI Involvement

DATA MANAGEMENT

- Data to POCC via HRM; no on-orbit recording
- Limited real time data available to AGCE GSE for accessing system performance and controlling the experiment:

  Temperatures

  Rotation Rate

  Voltage

  Marker Dot Location

  Scenario Number
- All data recorded by POCC for post mission analysis by PI

PS/PI INVOLVEMENT

- PS selects all experiment variables at start of each experiment scenario and initiates execution; experiment variables provided to PS in AGCE flight instrument document. No S/W stored scenarios.
- PI monitors experiment science status using AGCE GSE located at the POCC. PI controls duration of each scenario. Scenario terminated and new scenario start via voice instruction to PS from PI. PI may deviate from planned scenario sequence or change scenario parameters by voice instruction to PS (as long as planned peak power, data rates, total test time are not exceeded).

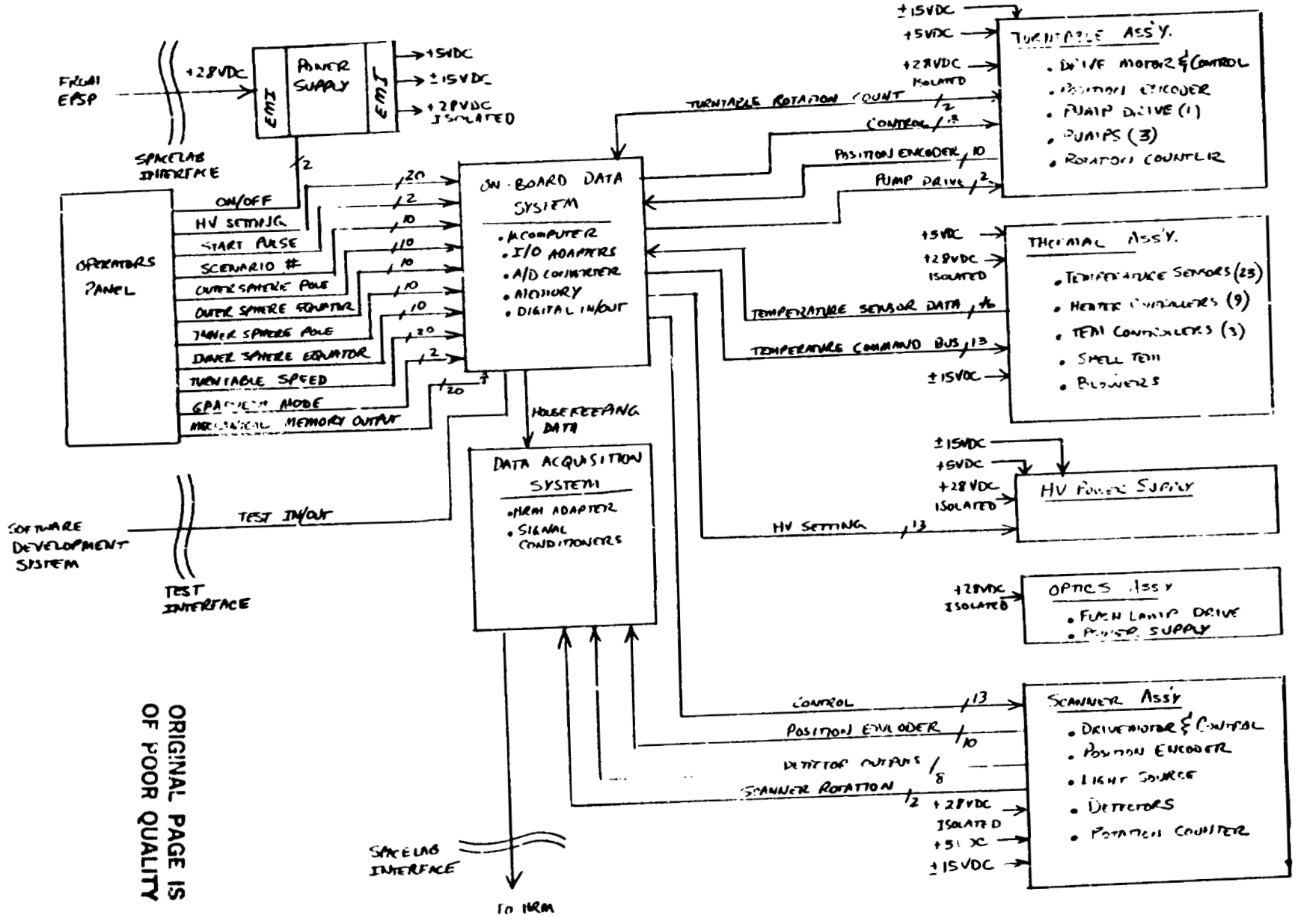

Figure 2.6-1. AGCE Electrical System Functional Block Diagram

Figures 2.6-2 and 2.6-3 show the on-board data system and data acquisition system portions of the electrical system. Figure 2.6-4 shows the end-to-end data path. The maximum data rate is estimated at 518.4 K bps. Note that time tagging using Greenwich Mean Time of AGCE telemetered data is not necessary and therefore not provided by the AGCE. This tagging can be provided by the POCC if desired. Time tagging at the POCC eliminates the need for an Remote Acquisition Unit (RAU) and RAU adapter as part of the AGCE flight system.

This overall experiment control and data handling philosophy is particularly well-suited to the nature of the implementation scheme selected for the AGCE. The approach not only lowers the cost of the flight unit but maximizes the use of the GSE and provides a high level of direct interaction by the principal investigator which is a necessary ingredient in the performance of a scientific experiment.

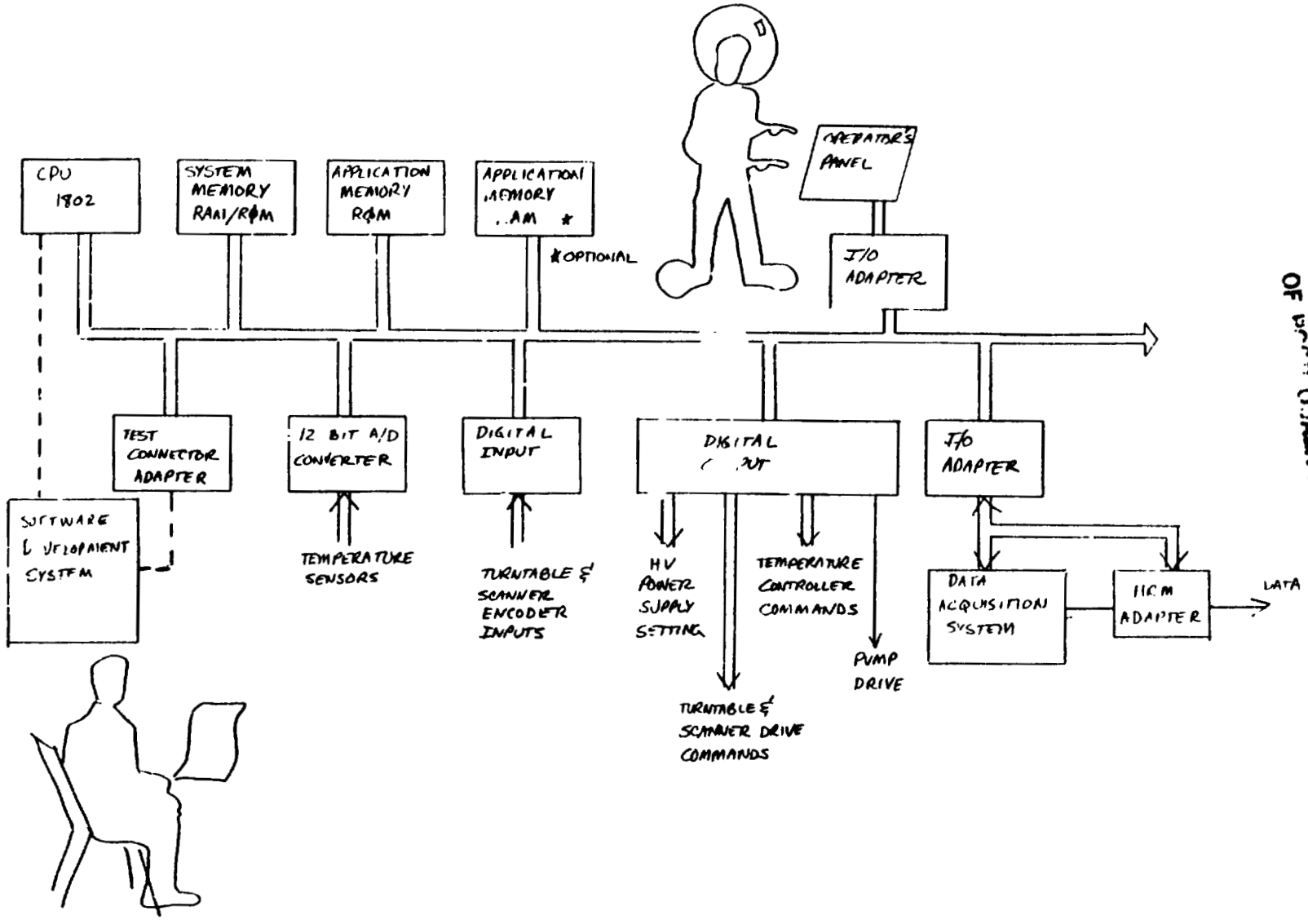

Figure 2.6-2. On-Board Data System Block Diagram

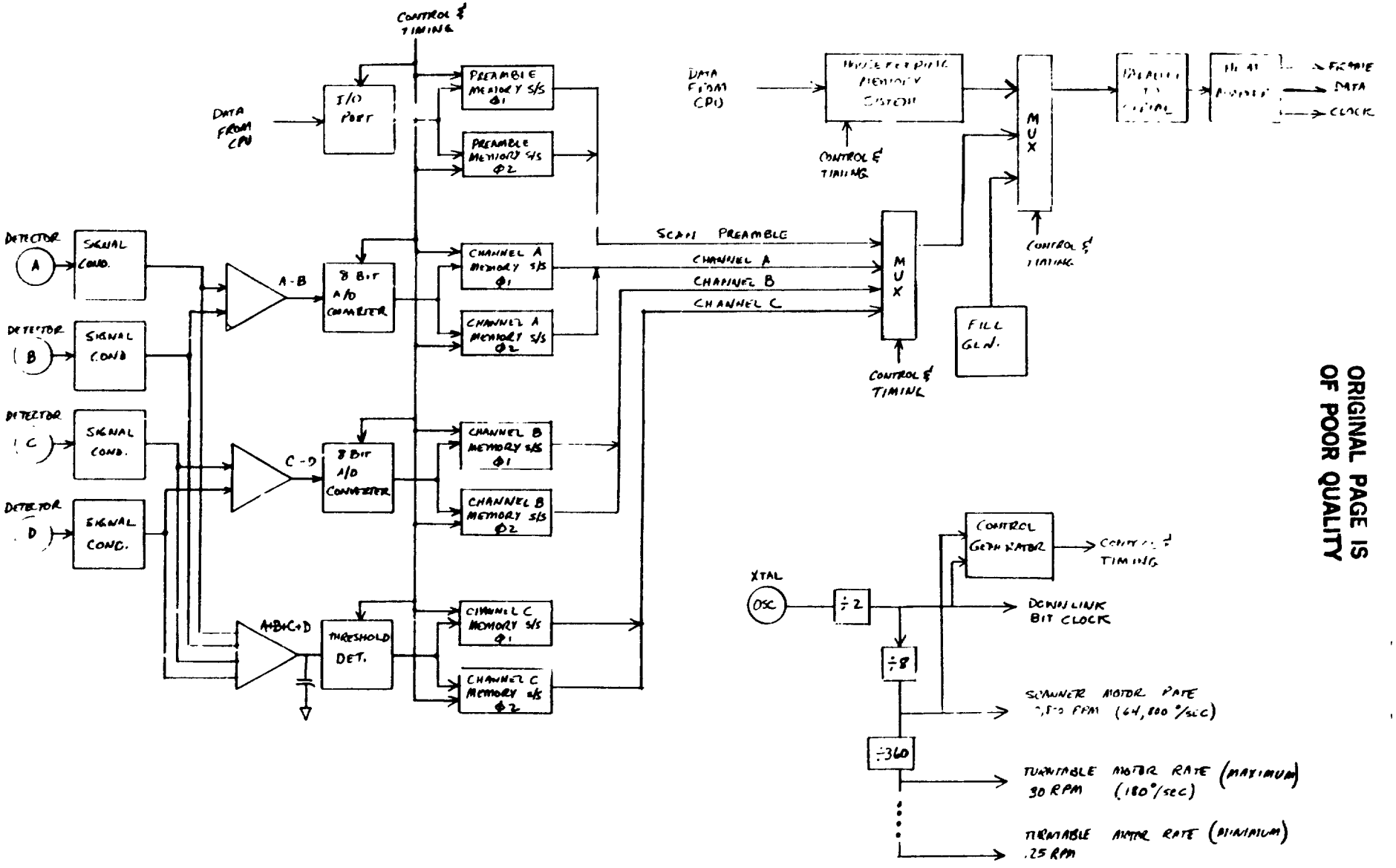

Figure 2.6-3. AGCE Data Acquisition System Block Diagram

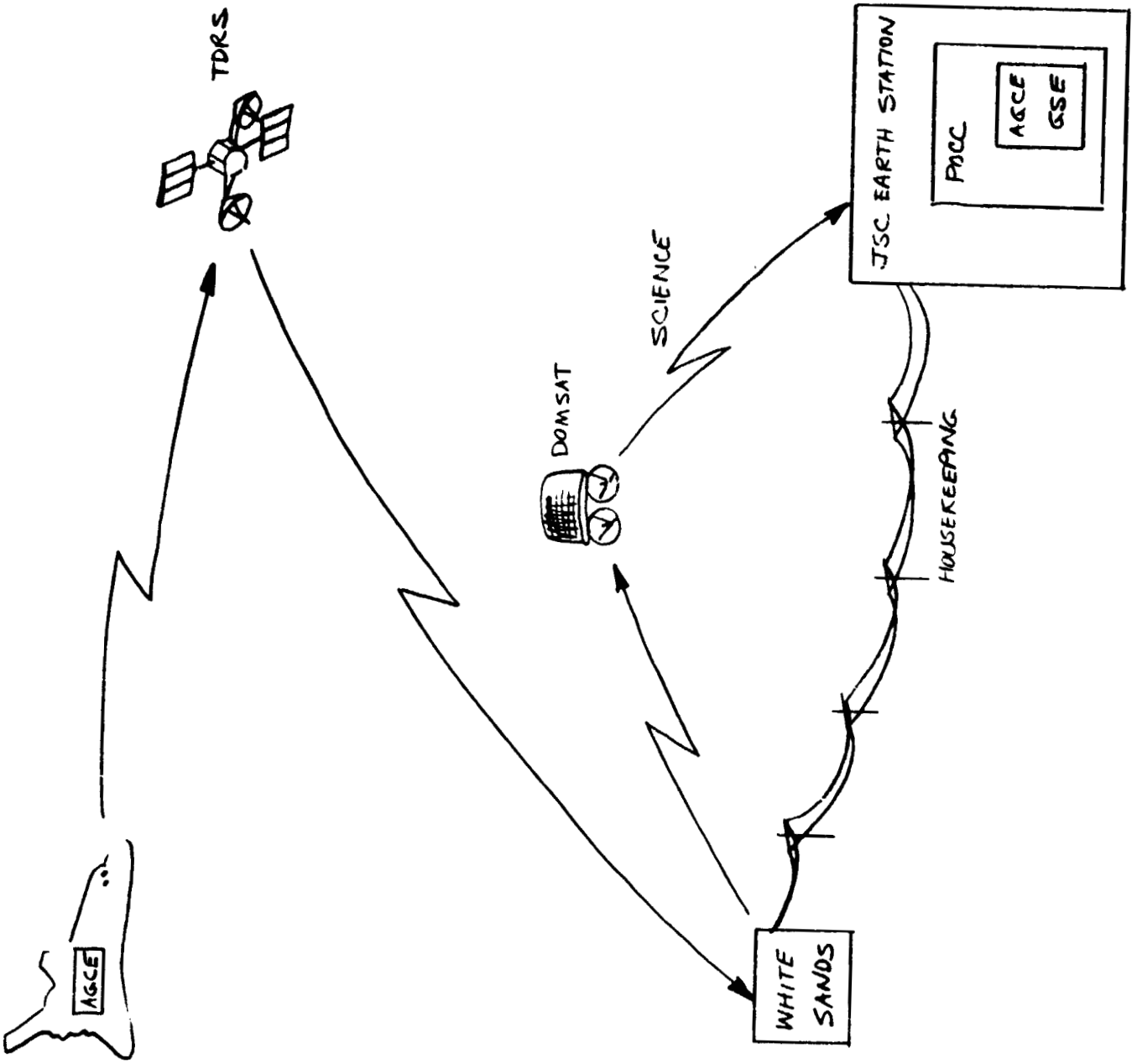

Figure 2.6-4. End-to-End Data System

2.7 APPARATUS CONFIGURATION

The general approach employed to generate the AGCE system configuration was to retain as much of the GFFC system configuration as possible and still be consistent with the new results generated during the course of this AGCE study. Configuration guidelines were also generated to assure compatibility with the Spacelab experiment area.

Although the AGCE and GFFC system configurations are fundamentally similar, implementation of some system features is found to be significantly different. This is particularly true in the areas of:

- Optics for experiment observations
- Flow cell construction
- Data management
- PS/PI/POCC involvement

However, wherever practical, the AGCE configuration is based on the corresponding portion of the GFFC system. For example, both systems use an air-to-air heat exchanger to transfer heat from the rotating turntable to the Spacelab's avionics air flow. Their design details are similar except that the AGCE turntable/heat exchanger combination is somewhat larger to accommodate the larger AGCE fluid flow cell.

The results of this configuration study clearly establish the feasibility of incorporating the AGCE into the Spacelab without any significant compromises to the experiment objectives and implementation schemes.

For the purpose of this configuration study, the AGCE system was assumed to provide the functions shown by Figure 2.7-1. As shown, the fluid flow cell is the heart of the system, simulating planetary or star conditions depending on

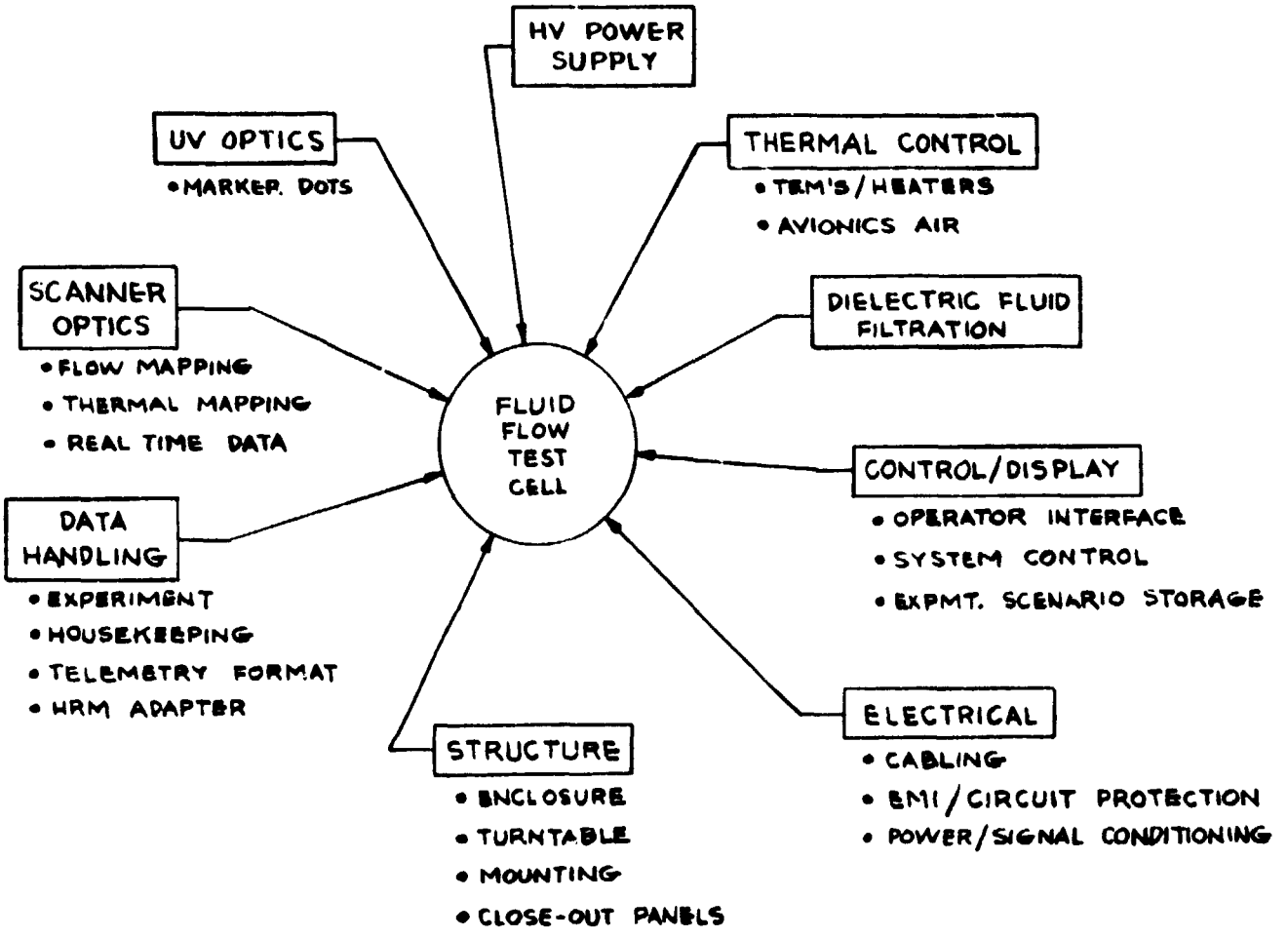

Figure 2.7-1. AGCE Functional Diagram

the direction of heat flow. System operation is initiated by the operator who selects and starts the desired experiment scenario. The microcomputer then issues commands in the appropriate time sequence to carry out the experiment scenario. Periodically, or at the beginning of each experiment scenario, the dielectric fluid in the flow cell is filtered to remove particulates. The thermal control capability establishes the desired thermal conditions on the inner and outer spheres of the flow cell (as well as transporting excess heat from all system elements to the Spacelab avionics air). High voltage is applied to the flow cell to simulate a gravitational field. The UV optics generates marker dots by activation of discrete areas in the dielectric fluid. The scanner optics generates real time data (in electronic form) for thermal and flow mapping of the dielectric fluid. This experiment data, and other housekeeping data, are formatted by the data handling electronics for transmission to the POCC via the Spacelab HRM.

Figure 2.7-2 shows the AGCE system installed in a simulated Spacelab single bay rack. Figure 2.7-3 displays the active interfaces with the Spacelab. The AGCE system can be contained within the dimensional envelope allowed by the Spacelab Payloads Accommodation Handbook SLP/2104. The AGCE system may be installed in either a single or double bay rack. A right hand side installation is preferred if a double bay rack is used, because the avionics air duct connections for the right hand side are identical to that for a single bay rack. Figure 2.7-4 shows the cabling diagram for the system.

Total AGCE flight system weight as shown in Table 2.7-1 is estimated at 104.3 kg. This estimate includes a growth contingency factor. The AGCE is comparable to the GFFC weight even though the AGCE cell is planned to be larger than used in the GFFC. The flow cell dimensions were selected to conform to the maximum

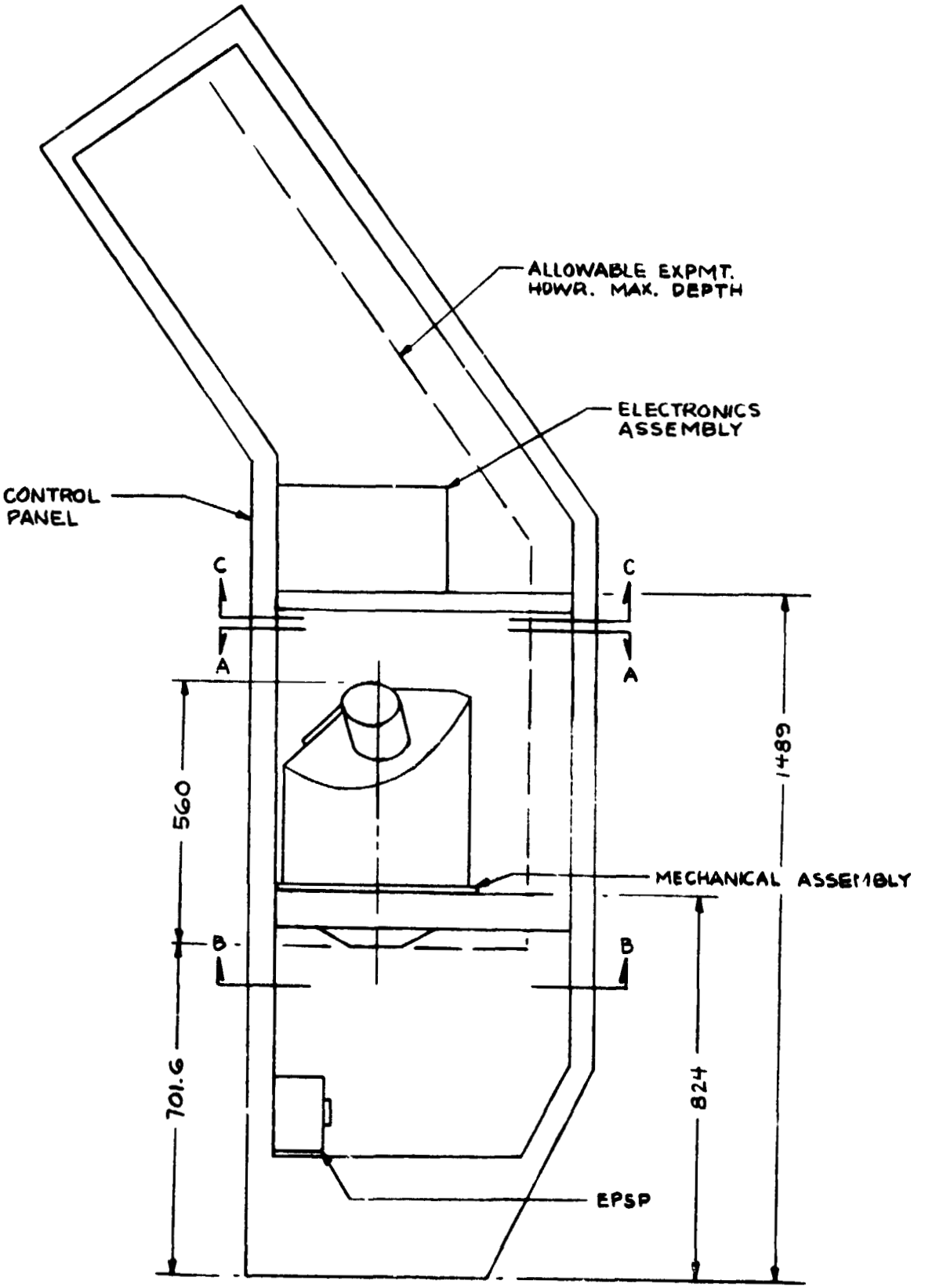

Figure 2.7-2. AGCE System Installed in Spacelab Rack
(CABLING, CLOSE-OUT PANELS, HOSE CONNECTIONS
TO AVIONICS AIR RETURN DUCT NOT SHOWN; DIMENSIONS IN MM)

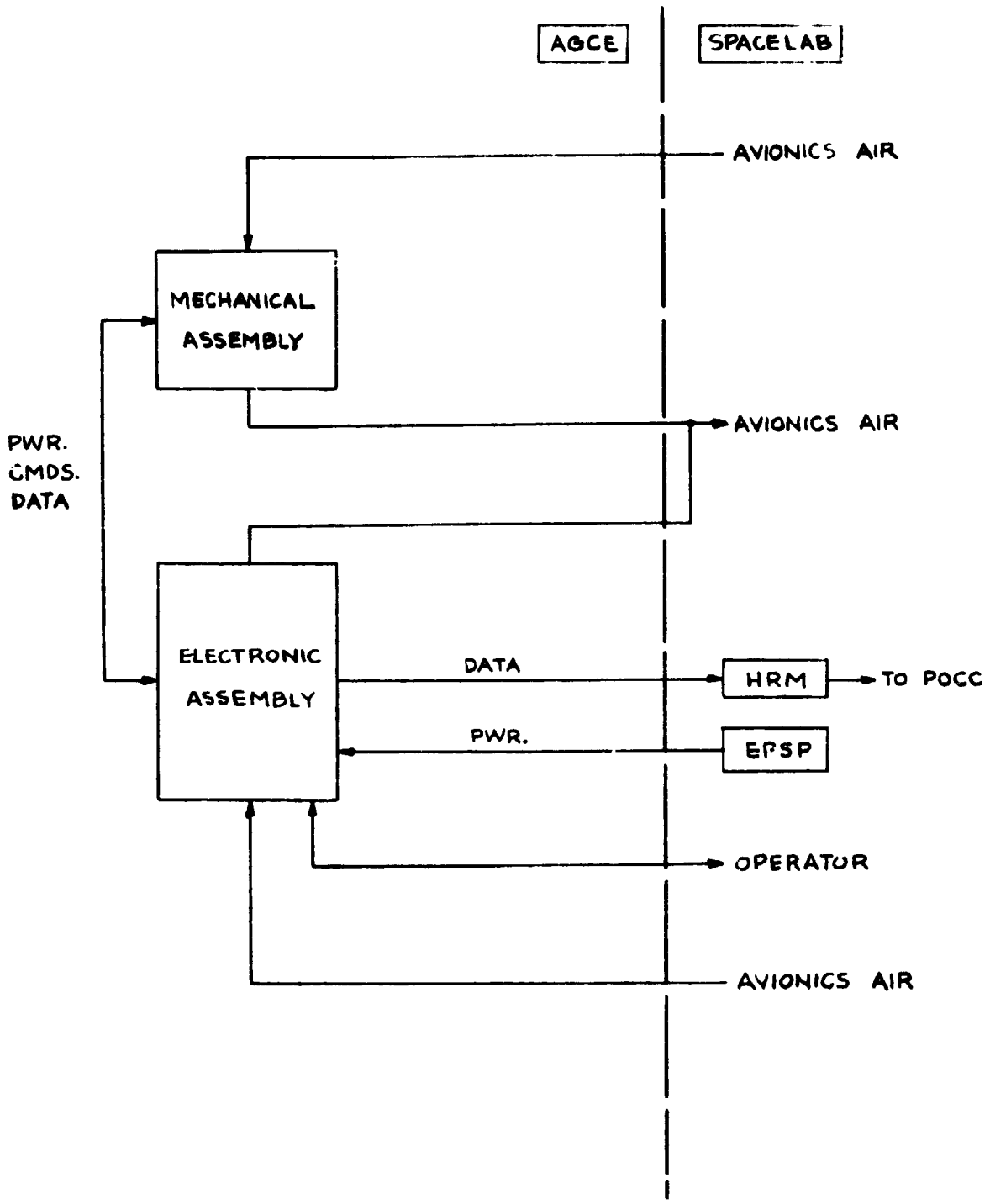

Figure 2.7-3. AGCE/Spacelab Interface Diagram

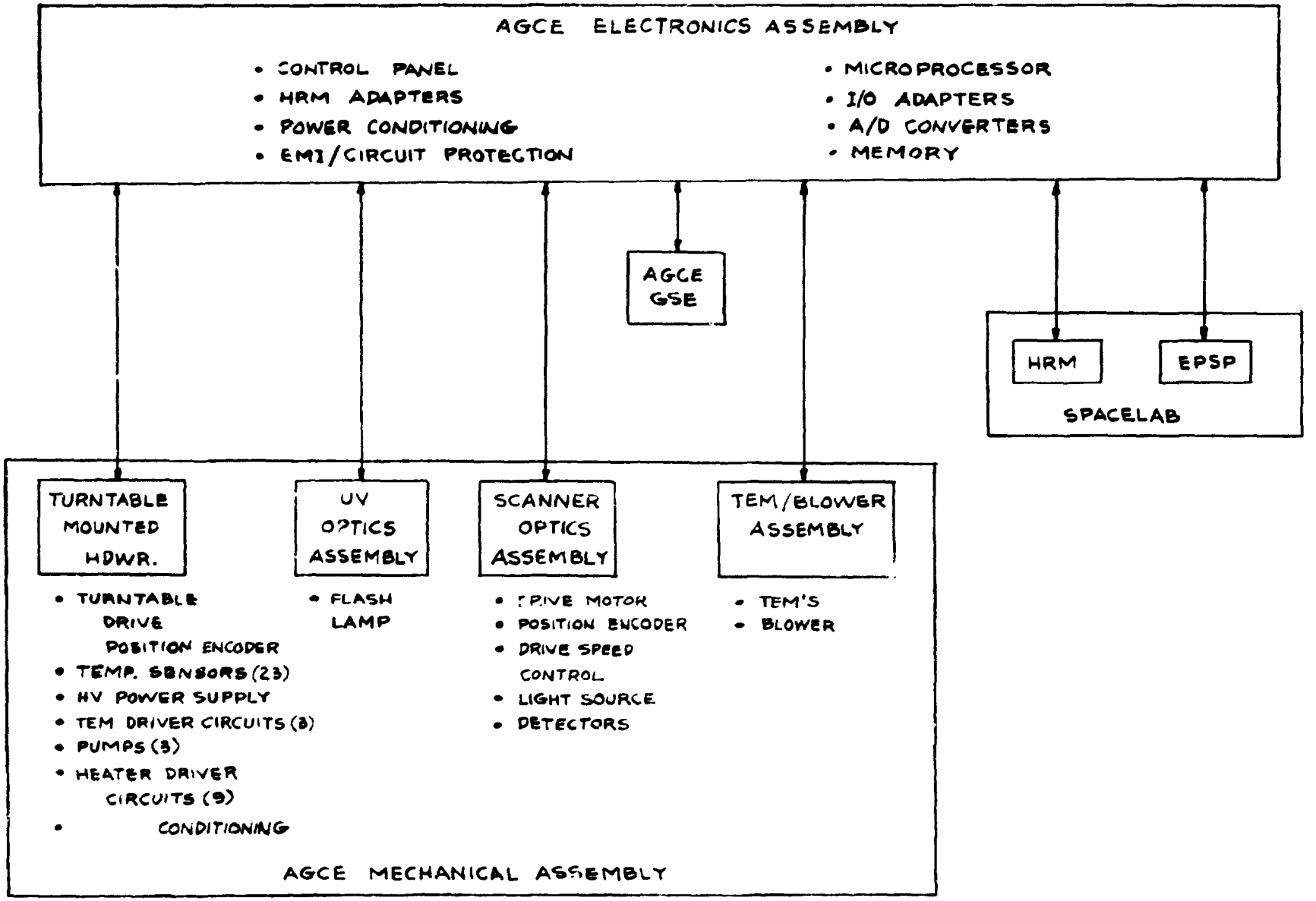

Figure 2.7-4. AGCE System Cabling Diagram

noted in the contract work statement, i.e. an inner sphere radius of 5.0 cm and an outer sphere inner radius of 6.0 cm. However, the mechanical assembly can accommodate a somewhat larger flow cell, on the order of 9.0 cm outer radius for the outer sphere (7.5 cm inner radius), with relatively minor impact.

Table 2.7-1

Estimated AGCE System Weight Compared with GFFC weight

System Element	AGCE Flight System	GFFC Flight System*
Mechanical Assembly	58.9 kg	66.6 kg
Electronic Assembly	31.7 kg	13.8 kg
Ancillary Equipment	13.7 kg	5.6 kg
Expendables	N/R	21.8 kg
TOTAL	104.3 kg	107.8 kg

*Data from GFFC IIA of 10/14/80

The details for each component of the AGCE were transferred to wooden models to examine relative placement and ease of access. The resulting wooden mock-up of the AGCF, described in Section 1.0, was found to be a useful visualization tool. Engineering sketches for the envelope were generated also during the course of the study and used to establish the physical characteristics important to both the configuration and cost estimation activities.

2.8 CONCLUSIONS AND RECOMMENDATIONS

The feasibility study for the Atmospheric General Circulation Experiment (AGCE) examined all of the technical areas critical to the successful implementation of the experiment on Spacelab. The overall conclusion to be drawn from the study results is that the AGCE is feasible for Spacelab with no identifiable technical obstacle to block its successful completion. Furthermore, the flexibility in the design parameters for the AGCE should be sufficient to permit good sensitivity in exploring the onset of baroclinic instabilities for terrestrial atmospheres.

The technical areas receiving the most attention in the study were: a) materials for the dielectric fluid, sphere shell, fluid baffle and contamination control; b) optical retrieval of experiment data; c) thermal control of experiment conditions; d) production of high voltages; and e) apparatus configuration and compatibility with Spacelab. These areas were recognized at the start of the program to be the most probable sources for limiting the feasibility of performing an adequate space experiment.

The results generated in each area did not uncover any insurmountable impediment to the AGCE. They did highlight however areas which must receive special attention in the final design of the AGCE to insure a successful experiment. Areas requiring extra attention include: a) purification, handling and maintenance of fluid quality for fluids with dielectric constants above 5; b) selection of materials coming in contact with the dielectric fluid to minimize contamination; c) processing procedures for the optical data to handle the effects of birefringence and target/detector rotation while scanning; d) scanner design to optimize the achievable signal-to-noise ratios necessary for good detection sensitivity of thermal gradients and fluid flow; and e) achievable heat exchange efficiencies at several interfaces within the experiment cell

which affect the control of thermal gradients and compatibility with mechanical interfaces. The analysis done in the study indicates each area can accommodate these concerns and will not limit, individually or collectively, the AGCE feasibility.

A significant conclusion to be drawn, when the results from the technical areas are considered collectively, concerns experiment flexibility. Sufficient variability exists in design parameters such as fluid dielectric constant, sphere cell diameter, experiment cell gap, range of thermal control and applied high voltage to allow considerable flexibility in establishing the experiment parameters. This flexibility can contribute significantly to adequately mapping conditions controlling baroclinic instabilities. The flexibility is further increased by the ability of the principal investigator to receive, evaluate and react in real-time to the AGCE results. This ability for the PI is achieved by the experiment control and data handling procedures selected for the AGCE.

The configuration for the AGCE fits well within a single experiment bay rack and can effectively mate with the services required for its operation.

The cost analysis for the AGCE does indicate a significant impact on total cost as a function of the starting date for the program. A minimum cost program therefore will require as early a start as possible.

The recommendations to be made lie principally in the realm of technical activities to insure a sound design with good performance margin. The recommendations of most significance are:

a) it is highly recommended that the fluid purification and characterization program outlined in this study be completed early in the AGCE final hardware design effort;

b) it is highly recommended that a general tolerance and sensitivity analysis for the system be done to establish limits on performance expectation and provide a basis for cost effective allocation of fabrication tolerances;

c) it is recommended that polarization of light in the optical scanner system be given further attention for data processing to accommodate birefringence and rotation affects;

d) it is recommended that further investigation be given to the selection and verification of heat transfer properties of the material to be used in the gap below the sphere's inner surface; this is most significant to achieving the predicted thermal control capability;

e) it is recommended that further investigation be done on the effective thermal conductance of the circular finned heat transfer module at the pole of the AGCE cell; this is most significant for configuration compatibility within the limited volume of the AGCE cell;

f) it is highly recommended that to minimize program cost, engineering design activity leading to an engineering model be initiated as early as possible.

☆ U S GOVERNMENT PRINTING OFFICE 1981—546-071/80